Project Title:	Integration of Behind-the-Meter PV Fleet Forecasts into Utility Grid System Operations
Project Period:	09/30/2013 – 12/31/2015
Submission Date:	02/26/2016
Recipient:	Clean Power Research, L.L.C.
Address:	1541 Third Street
	Napa, CA 94559
Website (if available)	www.cleanpower.com
Award Number:	DE-EE0006329
Project Team:	University of California, San Diego
	California ISO
	Itron
Principal Investigator:	Dr. Thomas Hoff, President Phone: 707-224-9992 Email: tomhoff@cleanpower.com
Business Contact:	Jennifer Gough, Project Manager Phone: 425-242-4174 ext. 7005 Email: jgough@cleanpower.com
HQ Tech Manager:	Rebecca Hott
HQ Project Officer:	Thomas Rueckert
GO Grant Specialist:	Christine Bing
GO Contracting Officer:	Daniel Scheulov

Executive Summary

Four major research objectives were completed over the course of this study. Three of the objectives were to evaluate three, new, state-of-the-art solar irradiance forecasting models. The fourth objective was to improve the California Independent System Operator's (ISO) load forecasts by integrating behind-the-meter (BTM) PV forecasts.

The three, new, state-of-the-art solar irradiance forecasting models included: the infrared (IR) satellite-based cloud motion vector (CMV) model; the WRF-SolarCA model and variants; and the Optimized Deep Machine Learning (ODML)-training model. The first two forecasting models targeted known weaknesses in current operational solar forecasts. They were benchmarked against existing operational numerical weather prediction (NWP) forecasts, visible satellite CMV forecasts, and measured PV plant power production. IR CMV, WRF-SolarCA, and ODML-training forecasting models all improved the forecast to a significant degree. Improvements varied depending on time of day, cloudiness index, and geographic location.

The fourth objective was to demonstrate that the California ISO's load forecasts could be improved by integrating BTM PV forecasts. This objective represented the project's most exciting and applicable gains. Operational BTM forecasts consisting of 200,000+ individual rooftop PV forecasts were delivered into the California ISO's real-time automated load forecasting (ALFS) environment. They were then evaluated side-by-side with operational load forecasts with no BTM-treatment. Overall, ALFS-BTM day-ahead (DA) forecasts performed better than baseline ALFS forecasts when compared to actual load data. Specifically, ALFS-BTM DA forecasts were observed to have the largest reduction of error during the afternoon on cloudy days. Shorter term 30 minute-ahead ALFS-BTM forecasts were shown to have less error under all sky conditions, especially during the morning time periods when traditional load forecasts often experience their largest uncertainties.

This work culminated in a GO decision being made by the California ISO to include zonal BTM forecasts into its operational load forecasting system. The California ISO's Manager of Short Term Forecasting, Jim Blatchford, summarized the research performed in this project with the following quote:

"The behind-the-meter (BTM) California ISO region forecasting research performed by Clean Power Research and sponsored by the Department of Energy's SUNRISE program was an opportunity to verify value and demonstrate improved load forecast capability. In 2016, the California ISO will be incorporating the BTM forecast into the Hour Ahead and Day Ahead load models to look for improvements in the overall load forecast accuracy as BTM PV capacity continues to grow."

Table of Contents

Background and Introduction

The penetration of customer-sited PV systems continues to grow as a result of reduced costs to the consumer, innovative business models such as third-party ownership and state-mandated renewable portfolio standards. This expansion of installed PV systems is increasing the amount of on-site energy generation leading to a change in the shape of the load profile during critical parts of the day. The California Independent System Operator (ISO) created the 'Duck Chart' to illustrate how the daily grid profile will change due to increasing penetrations of behind-the-meter (BTM) PV generation. Figure 1 illustrates these anticipated changes in California ISO load profiles. The increased penetration of PV impacts the capacity generation considerations for a utility. In addition, it does this inconsistently across hours of the day or day of the year. This is because PV generation is variable by nature across multiple time domains: the production of a fleet of PV systems may not produce the same amount of energy today as it did yesterday.

California ISO and utilities will need to balance the swings in "net load" caused by the variability in solar generation by scheduling reserve resources with increasingly steep ramp rates and increasing associated costs. The net load profile presents an additional ramp-down in the morning and a bigger, steeper ramp-up before peak load in the evening. The magnitude of these additional ramps will only increase as additional BTM PV systems are installed. The absolute accuracy of current load prediction methods will continue to decrease as overall PV capacity grows within a balancing area. This will have a direct impact on the California ISO's ability to manage and purchase reserve capacity.
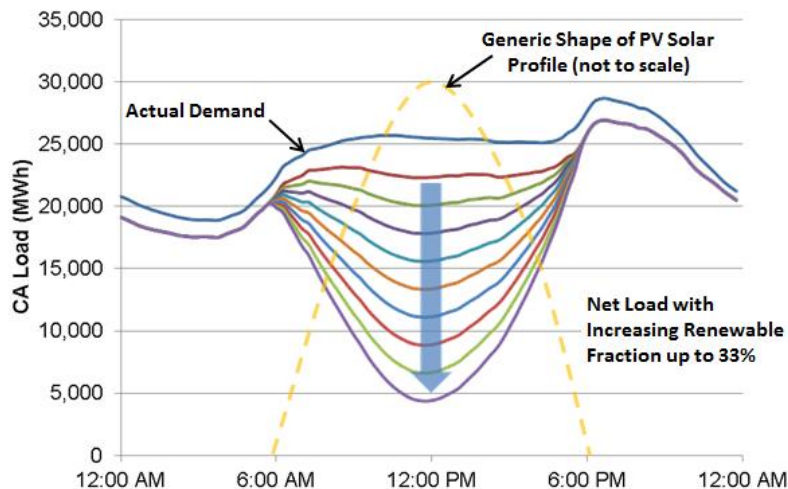
Figure 1: An example of predicted California ISO load profile changes (a.k.a. the Duck Curve) as higher penetrations of renewable energy (primarily solar) are installed on the grid. A typical profile of BTM PV production is shown in yellow (dashed).

Forecasting production of PV systems, however, is not completely uncertain and can be predicted along the known daylight hours. Fundamentally, PV production forecasts are heavily reliant on the ability to predict cloud cover. Accurate prediction requires a good

understanding of spatial cloud correlation and movement and generation, which must be factored into operational PV production forecasts.

The Need for Site-Specific BTM Forecasting

No commercially-available product exists that explicitly forecasts distributed BTM PV energy production as an offset to balancing area load scheduling. The need for this capability is driven by the increasing number of PV systems coming online coupled with the lack of generation correlation between adjacent distributed PV sites. Utilities and ISOs have limited budgets and personnel resources available to address this growing problem. Thus a scalable, cost-effective method for operational improvements is required.

One existing solution is to use persistence methods of load prediction that heavily weight recent day usage. This solution, however, can cause difficulties when a cloudy day precedes a sunny day throughout most of the utility coverage area or vice-versa. A persistence-based approach will over-predict the customer load on the first day and over compensate and under-predict the customer load on the following day.

Another existing solution (Tuohy et al.) is to assume a total BTM PV capacity over a large geographic area and to forecast production as a "single" PV system. Figure 2 presents the current California distributed PV generation capacity. It shows that there is a wide variety of system sizes and disbursed locations. In addition, there are a variety of system orientations. It is challenging to aggregate such a diverse set of systems. This method also over simplifies the challenges in cloud patterns centered on their low spatial correlation during variable irradiance (e.g., partly cloudy) conditions.

Both solutions will lead to unsustainable forecasted load errors and higher PV integration costs as PV capacity increases.
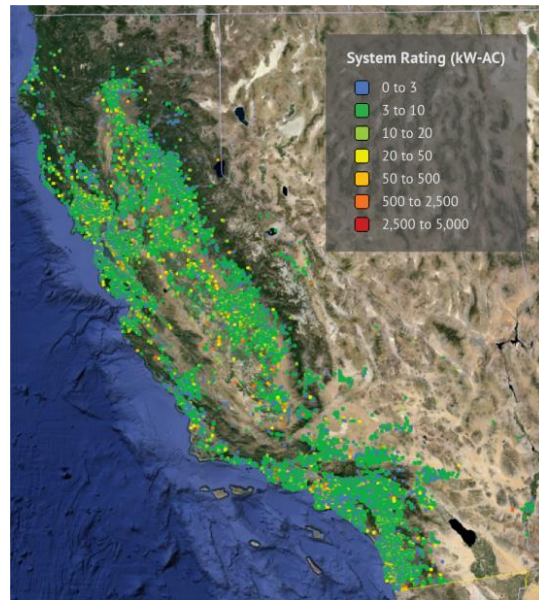
System Rating (kW-AC)
- 0 to 3
- 3 to 10
- 10 to 20
- 20 to 50
- 50 to 500
- 500 to 2,500
- 2,500 to 5,000

Figure 2: Distribution and capacity of BTM PV systems throughout California.

This project successfully integrated state-of-the-art forecasting methods into the largest U.S. solar market (currently nearly 40% of the nationwide solar generation occurs in California) to yield robust and accurate forecast products for an important stakeholder, the California ISO. The California ISO is charged with maintaining the reliability and accessibility of operation for the region's electricity grids. Its balancing area covers zones serviced by three of the largest US investor-owned utilities (PG&E, SCE and SDG&E), all of which are experiencing rapidly increasing numbers of BTM PV systems.

The solution is provided through a software service that predicts BTM PV generation using a combination of satellite and numerical weather prediction (NWP)-based irradiance forecasting methods and widely accepted PV system energy simulation algorithms. This solution is embodied in the software product SolarAnywhere® FleetView®.

FleetView enables the generation of a seven-day forecast for every unique PV system and the aggregation of forecasted generation, by utility or ISO-relevant grouping. FleetView provides a significantly more precise approach to estimating the offset to utility load due to BTM PV generation when compared with existing methods.

Building on Prior Knowledge

This project's success is due to the existing work performed between Clean Power Research (CPR) and the California ISO. Previous work focused on developing the algorithms and framework needed to facilitate BTM forecasts. A primary task of this project was to integrate these BTM PV forecasts, for all PV systems within the state of California, into the California ISO Short Term Forecasting Group's Automatic Load Forecasting System (ALFS). A task which ties directly to the overall goal of improving both the hour-ahead and day-ahead California ISO load forecasts. Additionally, metered

utility owned PV system data was used to evaluate existing forecast accuracy and enable the application of further forecast improvements developed by University of California, San Diego (UCSD). The successful integration of an operational BTM PV generation forecast into load planning and operational tools for the California ISO has established an approach that other areas of the country could follow.

The results presented in this report are focused on the summary of overall project tasks listed in Table 1.

Table 1: Table of overall project tasks, milestones and deliverables.

Task 1	Integrate FleetView Forecasts into the California ISO Generation and Load Scheduling and Real-Time Operations	
Budget Period 1		
Subtask *(BP1)*		
1.1	Understand how the California ISO uses load forecasts in their balancing operations	
1.2	Design features in FleetView to meet the use of California ISO	
1.3	Build in the desired feature set to FleetView	
Deliverable *(BP1)*		
1.1	Specification document of data format for importing fleet forecasting into California ISO ALFS	*Achieved*
1.2	Specification document of communication protocol for importing fleet forecasting into California ISO ALFS	*Achieved*
1.3	Summary document that presents results from completion of Task 1 and focuses on repeatable methods for integrating FleetView forecasting software with any utility load forecasting tool	*Achieved*
Milestone *(BP1)*		
1.1	CPR will deliver FleetView forecasts into the California ISO ALFS in time for the information to be operationally relevant, based on the feedback from the California ISO in Deliverables 1.1 – 1.3	*Achieved*

Task 2	Improve Forecast by Integrating High Resolution (4-km grid, 15-minute output out to 24 hours in forecast horizon) Numerical Weather Prediction (NWP) Model and Optimized Deep Machine Learning (ODML) method forecasts into FleetView	
Budget Period 1		
Subtask (BP1)		
2.1	Generate a specification outlining important parameters in generating and integrating advanced solar forecasting methods, Weather Research and Forecasting (WRF-SolarCA)	
2.2	UCSD will generate WRF-SolarCA model forecasts for specific regions and time domains	
2.3	CPR will generate new infrared satellite image forecasts for specific regions and time domains	

2.4	Generate a specification outlining data transfer requirements to properly operate the ODML method from Prof. Carlos Coimbra	
Deliverable (BP1)		
2.1	Specification document defining the optimal configuration for UCSD WRF-SolarCA model forecast improvements	*Achieved*
2.2	Specification document defining the information flow connecting all unique forecasts with the ODML methods developed by Prof. Carlos Coimbra	*Achieved*
Milestone (BP1)		
2.1	UCSD will produce and deliver to CPR forecast outputs based on the WRF-SolarCA model as defined by the document in Deliverable 2.1	*Achieved*
2.2	UCSD will produce and deliver to CPR forecast output based on the ODML methods as defined by the document from Deliverable 2.2	*Achieved*
Budget Period 2		
Subtask (BP2)		
2.5a	Produce an optimal ODML-based forecast at 52 California ISO metered PV locations	
2.5b	Re-configure the WRF-SolarCA model using BP1 results to generate model output in a California climate region	
2.6	CPR will integrate forecast improvements into FleetView	
Milestone (BP2)		
2.4	Go/No Go decision by the California ISO whether to integrate FleetView forecasts into their operational ALFS.	*Achieved*
2.5	FleetView forecasts will be optimized for computational performance to deliver information to the California ISO ALFS at an average time of 20-minutes +/- 7-minute standard deviation	*Achieved*

Task 3	**Validate FleetView Forecast Accuracy against Metered California ISO Data**	
Budget Period 1		
Subtask		
3.1	Acquire metered PV system data for the utility scale plants from the California ISO	
3.2	Quantify the accuracy and subsequent value of the FleetView forecasts	
3.3	Quantify the accuracy and subsequent value of advanced forecasting techniques	
Deliverable		
3.1	Summary document that presents the results of comparing the accuracy of FleetView plant specific forecasts with the California ISO ground data for the 52 metered PV systems	*Achieved*
3.2	An accuracy summary document highlighting the relative improvements of FleetView forecasts and highlighting particular areas of improvement, including geographic region, climate conditions and relative PV penetration level	*Achieved*
3.3	California ISO ground data delivered to CPR for 52 total metered PV systems over the period of 2014 for four-second interval measurements	*Achieved*
Milestone		

3.1	California ISO ground data delivered to CPR for 52 total metered PV systems over the period of 2013 for four-second interval measurements	*Achieved*
3.2	CPR will produce early morning forecasts using satellite infrared channel images by developing research methods	*Achieved*
Budget Period 2		
Subtask		
3.2	Quantify the accuracy and subsequent value of the FleetView forecasts while providing the California ISO feedback on forecast accuracy	
3.3	Quantify the accuracy and subsequent value of advanced forecasting techniques to drive decisions on whether to add the forecasting technique to the existing FleetView forecast service and provide a basis for the California ISO to understand where the FleetView forecasts are most effective, either in a locational, seasonal or diurnal framework	
Milestone		
3.3	Summary document that presents the results of comparing the accuracy of existing FleetView plant specific forecasts and newly added forecast improvements with the California ISO ground data for the 52 metered PV systems, as noted in Milestone 3.3	*Achieved*

Task 4	Quantify Impact of FleetView Forecast on Improved California ISO Load Forecasting	
Budget Period 1		
Subtask		
4.1	Acquire metered forecast and actual load data for the desired geographic zones from the California ISO	
4.2	Quantify the accuracy and subsequent value of the FleetView forecasts	
4.3	Quantify the accuracy and subsequent value of advanced forecasting techniques	
Deliverable		
4.1	Summary document that presents the results of comparing the accuracy of existing California ISO ALFS load forecasts to actual system load with and without incorporating FleetView behind-the-meter forecasts	*Delayed to BP2*
4.2	Summary roll out presentation of all Budget Period 1 deliverables to select stakeholders and the Department of Energy	*Achieved*
Milestone		
4.1	California ISO forecast and actual load data delivered to CPR for five defined geographic zones over the time period 2013 at 4-second intervals	*Delayed to BP2*
Budget Period 2		
Subtask		
4.2	Quantify the accuracy and subsequent value of the FleetView forecasts	
Milestone		
4.2	Summary document that presents the results of comparing the accuracy of existing California ISO ALFS load forecasts to actual system load with FleetView behind-the-meter forecasts	*Achieved*

| 4.3 | CPR will submit abstract and apply to present at one or more technical conferences, where results from the project will be presented to the research community | *Achieved* |

Task 5	Provide DOE and Public Accessible Data Created from this Project	
	Budget Period 1	
Deliverable		
5.1	All data generated as part of the scope of this project in Budget Period 1 in easily viewed and downloadable format no later than 30 days after the conclusion of Budget Period 1	*Achieved*
	Budget Period 2	
Milestone		
5.2	All data that was generated as part of the scope of this project in Budget Period 2 in easily viewed and downloadable format no later than 30 days after the conclusion of Budget Period 2	*Achieved*

Task 6	Dissemination, Replication and Impact of EERE funding	
	Budget Period 2	
	Lessons learned from data sharing and the simulations of high-renewable penetration scenarios will be shared with the broader power system operators' stakeholder group by coordinating with DOE's other parallel activities as appropriate	

BP1	Go/No Go Decision	
	At the end of Budget Period 1, a Go/No Go Decision will be made based on successful completion of 85% of BP1 subtasks and deliverables	*Achieved*

Project Results and Discussion

Integration of FleetView Forecasts into the California ISO Real-Time Operations (Task 1 Highlights)

Under this project, FleetView BTM forecasts were extended, operated, and demonstrated for a period of two years. FleetView has been reliably providing ten separate fleet forecasts to the California ISO for Day Ahead Market and Real-Time Pre-Dispatch needs. This operating experience has enabled CPR to work through technical challenges and demonstrate a working BTM forecasting system.

Zonal FleetView BTM forecasts are now fully integrated into the California ISO operational environment. Integration includes both forecast delivery (via secure FTP as pre-arranged with the operator) as well as dynamic feedback (also over FTP). This system meets all security requirements and has proven to be highly robust and reliable. This effort was undertaken to meet subtasks 1.1-1.3.

Satellite-based Forecast Improvements (Task 2 Highlights)

Satellite CMV Forecast Model

CPR's satellite-to-irradiance model forms the crux of satellite cloud motion vector (CMV) forecasts. The CMV forecast model has been updated to utilize Geostationary Operational Environmental Satellite (GOES) infrared (IR) channels. This update enables the CMV forecast model to detect pre-sunrise clouds and subsequent cloud motion. The IR CMV model produces forecasts from pre-sunrise onward. This capability was not present in the visible satellite channel-only CMV model.

Figure 4: SolarAnywhere satellite-based power forecasting process flowchart.
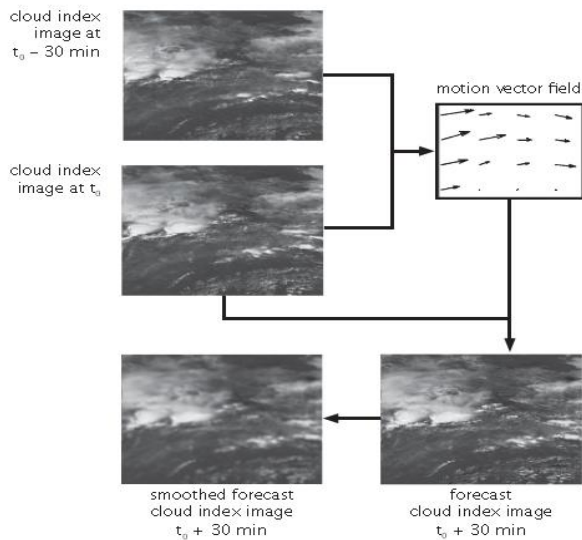
Figure 3: Example CMV technique derived from two consecutive visible satellite images (from Lorenz et al., 2004). Infrared-based CMV forecasts are derived in a similar fashion from consecutive IR satellite images.
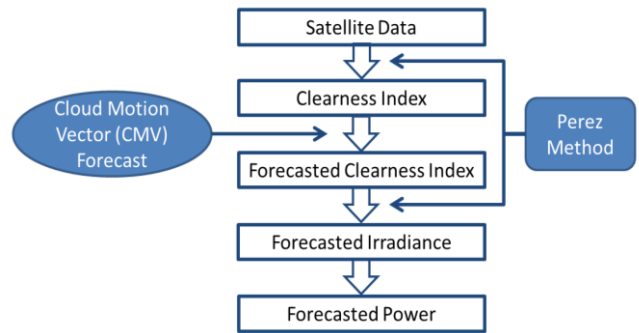
Short-term irradiance forecasts are produced using consecutive GOES 1-km visible and 4-km IR satellite images to infer cloud motion as illustrated in Figure 3. CMVs are determined by minimizing the error of the difference between consecutive satellite image-derived clearness index maps. Clearness index maps for subsequent hours, up to 5 hours ahead, are derived from the localized motion of individual pixels. A pixel-specific clearness index is advected in the direction of the CMV determined for the considered location. The considered location is also assigned the clearness index value of the pixel upstream from the target location.

A steady state cloud supposition is made during the satellite-based forecast period during which no cloud growth or decay occurs. Future images are subsequently smoothed following the approach described by Hammer et al. (2001). The final translation from clearness index to irradiance is then performed via the Perez et al. (2002) method. The overall GOES satellite-based forecast process is diagrammed in Figure 4.

IR CMV model forecast results are generally less accurate than concurrent visible CMV forecast model results due to the lower resolution of the IR channel source data and to challenges inherent to IR channel cloud detection.

NDFD model forecasts

SolarAnywhere short-to-medium term solar irradiance forecasts are derived from the National Digital Forecasting Database (NDFD) gridded cloud forecasts following a methodology similar to short-term satellite-based forecasts. The NDFD cloud amount products are the result of a multiphase forecasting process. The process involves: (1) prediction of global forecasts using NWP; (2) modification of the global forecasts by regional meteorological offices using tools that include mesoscale models and human input; and (3) reassembling of the regional offices' products into a national grid. The cloud-amount-to-irradiance procedure is adjusted empirically to better match the ensemble of observations at regionally appropriate ground locations, particularly to account for a tendency towards cloud amount under prediction as NWP forecast time horizons increase. Further details about the NDFD model can be found at the flowing URL: http://www.nws.noaa.gov/ndfd/. Pre-dawn solar forecasts in SolarAnywhere currently rely on NDFD model due to the lack of visible GOES satellite imagery.

Translation to PV Power

FleetView explicitly models the translation of irradiance to PV power. This is one key differentiator of FleetView versus other approaches. Site-specific irradiance (GHI and DNI), temperature and wind speed data along with PV site details (module type, inverter type, row spacing, tilt angle, DC/AC size, etc.) are incorporated together and fed into a PV performance model as illustrated in Figure 5. FleetView was designed specifically

for solar energy and thus has been developed with this more accurate approach. This is opposed to other irradiance-to-power scaling or correlation techniques (e.g., model output statistics (MOS) or measure-correlate-predict) ported over to the solar industry from wind forecasting techniques. Accurate PV system configuration specifications can
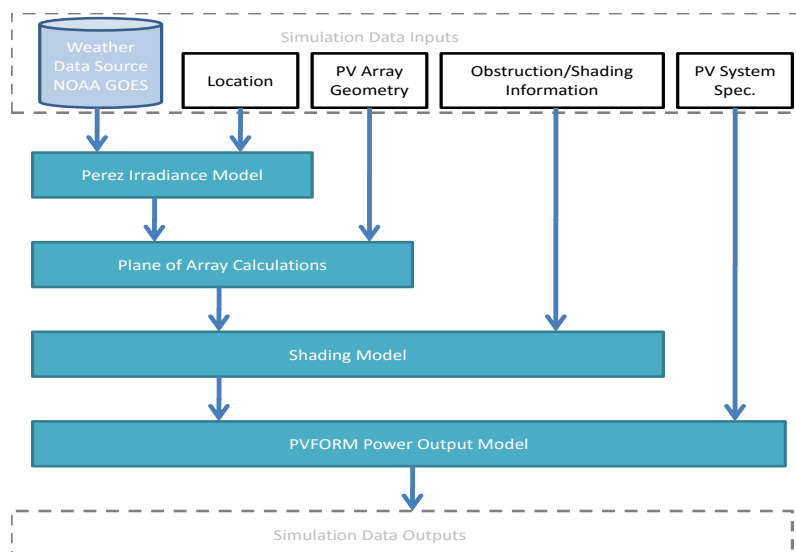

Figure 5: PV simulation architecture within FleetView.

impact overall system power forecast accuracy as much as the underlying irradiance data. The translation to power is the last step of the overall solar energy forecasting process.

Forecast Evaluation Methodology and Metrics

All forecasts evaluated for this project are validated against corresponding hourly quality controlled irradiance and PV plant production data. Error metrics reported include Mean Bias Error (MBE), Mean Absolute Error (MAE), Mean Absolute Percent Error (MAPE) normalized by capacity, and Root Mean Square Error (RMSE). Each of these 4 error metrics are defined below:

$$MBE = \frac{\sum_{i=1}^{n}(F_i - O_i)}{n}$$

$$MAE = \frac{\sum_{i=1}^{n}(|F_i - O_i|)}{n}$$

$$MAPE = \frac{MAE}{Capacity}$$

$$RMSE = \sqrt{\frac{\sum_{i=1}^{n}(F_i - O_i)^2}{n}}$$

where F_i is forecasted, O_i is observed. Nighttime values have been excluded from reported error metrics.

Solar PV Plant Data and Cleaning

Production PV data were accessed for 52 metered PV plants located throughout the California ISO balancing zone for the time period spanning May 2014 through May 2015. Hour averages of one-minute resolution PI data were cleaned and stored for future use. Metered PV sites with significant suspicious data were removed from consideration. Additionally, co-located PV sites were removed from consideration due to the duplicate nature of the resulting forecast metrics. Twenty of the initial 52 sites were removed due to the aforementioned cleaning factors.

The locations of the remaining 32 PV plants are presented in Figure 6. They can be grouped into climate-specific regions in California. PV sites evaluated include 2 sites in Bay Area (BA), 14 sites in Los Angeles (LA), 5 sites in Desert (D) and 11 sites in San Joaquin Valley (SJV). These regions represent the coastal, inland valley and desert climate regions of California, that compose solar energy forecast regions relevant to the California ISO.
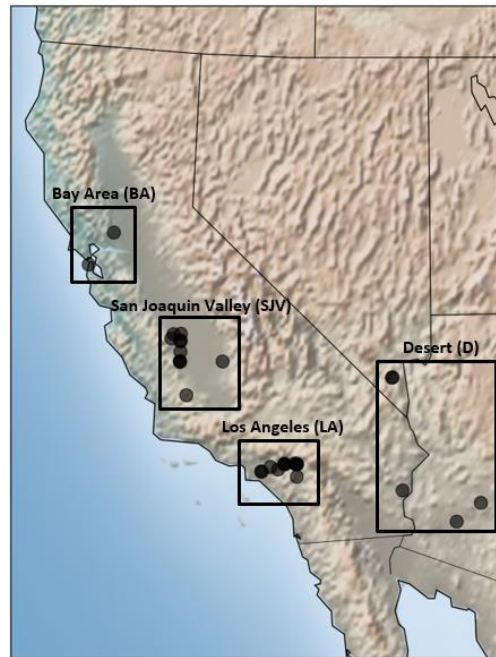
Figure 6: Map of 32 Utility-scale PV solar plant locations evaluated in this report. PV solar sites are grouped into 4 solar energy forecast regions used to aggregate individual PV plant forecast results. These regions include the Bay Area (BA), San Joaquin Valley (SJV), Desert (D) and Los Angeles (LA).

IR CMV Model Forecast Results

Figure 7 presents IR and visible CMV forecasts for a PV site located in the Desert region. The figure shows that IR CMV forecasts provide operational coverage well before the availability of visible CMV forecasts (9 AM LST in this example). The underlying NDFD forecast predicted clear skies during the morning while the pre-dawn IR CMV forecasts accurately predicted suppressed PV power production due to cloud cover.
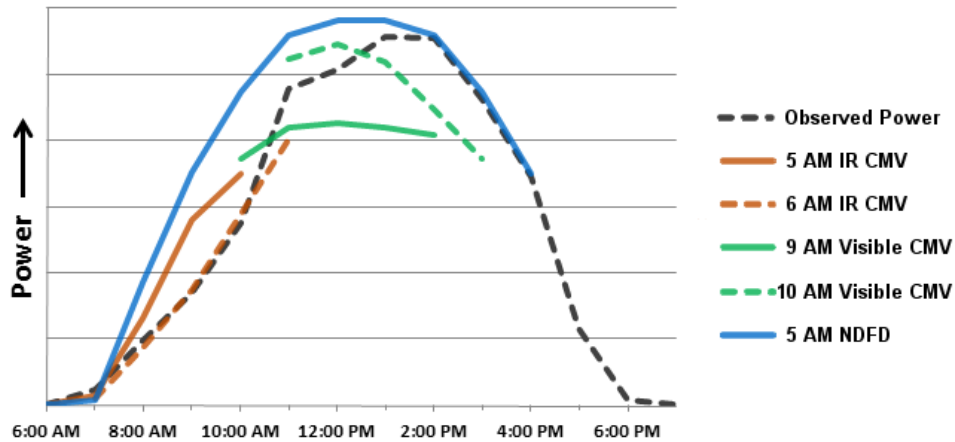

Figure 7: (IR CMV, visible CMV, and NDFD PV energy forecasts on February 19th, 2015 for a Desert region location. Ground observations of PV power are shown for validation purposes.

Individual PV site power forecasts consisting of IR CMV and NDFD model forecasts are analyzed at all four California regions over a thirteen-month period spanning May, 2014 through May, 2015.

Figure 8 presents the annual averaged errors resulting from time-specific forecasts for a SJV region PV site. The figure suggests that forecast accuracy is improved under cloudy sky conditions with either the pre-dawn IR CMV forecasts or the post-dawn visible CMV forecasts when compared to the NDFD forecasts. Clear sky forecast errors are very similar in nature and shape at all SJV locations.

Figure 9 suggests that seasonal impacts on forecast accuracy are stronger during the winter months. This is likely due to increased cloud cover from Pacific frontal weather systems and the morning occurrence of Tule Valley fog.
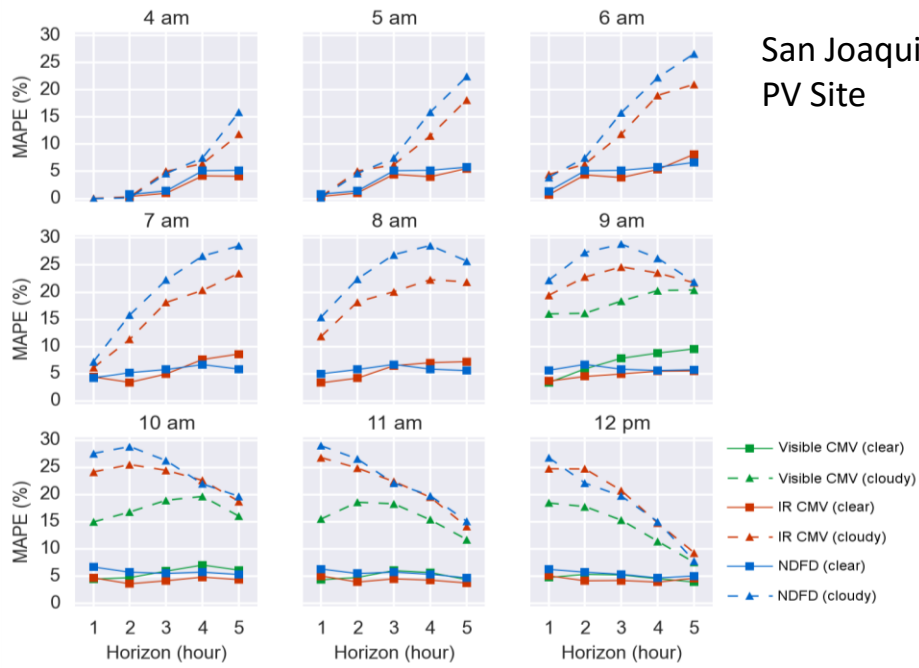
Figure 8: Annual SJV PV site forecasting error statistics (MAPE) shown for cloudy (dashed lines) and clear (solid lines) observed sky conditions. Error metrics are reported by forecast horizon (1-5 hours) for forecasts initialized at 4 AM through 12 PM (top left to lower right).
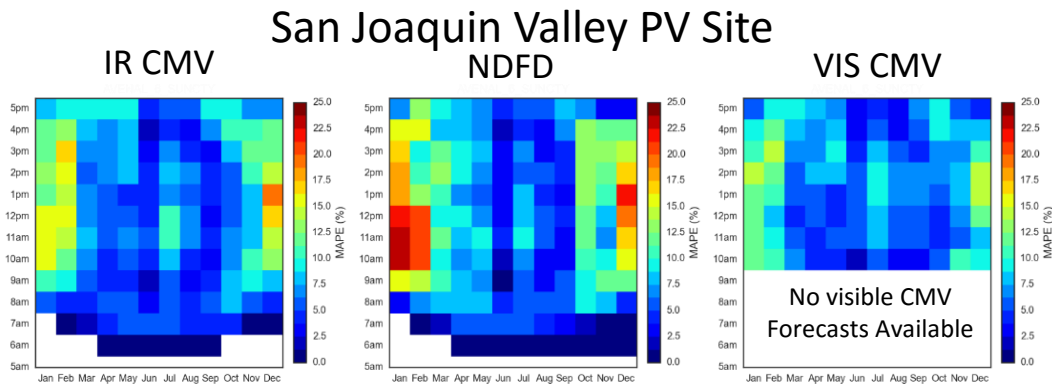
Figure 9: Seasonal forecasting error statistics (MAPE) for the single SJV PV site. Hourly forecasts illustrated in Figure 7 are averaged per hour and aggregated monthly to emphasize seasonal forecast error patterns under all sky conditions.

Regional Aggregate PV Site Forecast Results

Table 2 reports aggregate pre-dawn power forecast error statistics for the four regions. Inspection of the forecast results shows improvement in IR CMV forecasts at PV sites located at both inland California regions (D and SJV) under all sky conditions, but not at PV sites located in the two coastal regions (BA and LA). This is likely due to IR CMV

model limitations when low level marine stratus clouds are present and will be elaborated on further in the next section.

Table 2: Error metrics for IR CMV and NDFD forecasts spanning 13 months (5/2014 – 5/2015). Aggregate regional PV power forecasts generated at 5 and 6 AM LST spanning the 1-4 hour ahead forecast horizon are included in the error analysis.

Forecasts		Bay Area (BA)			Los Angeles (LA)		
		All	Clear Sky	Cloudy	All	Clear Sky	Cloudy
MBPE (%)	IR	4.80	-1.88	9.19	5.74	-0.38	10.97
	NDFD	0.73	-3.31	3.70	1.79	-1.71	5.06
MAE (%)	IR	7.91	3.72	9.92	8.29	3.99	11.61
	NDFD	6.40	5.26	7.38	7.78	5.50	10.12
RMSE (%)	IR	10.76	5.13	12.53	11.35	5.11	14.45
	NDFD	9.02	7.78	9.79	10.69	8.20	12.43
Forecasts		Desert (D)			San Joaquin Valley (SJV)		
		All	Clear Sky	Cloudy	All	Clear Sky	Cloudy
MBPE (%)	IR	1.73	-0.45	6.02	1.19	-2.63	7.58
	NDFD	2.39	0.29	5.70	2.18	-1.07	7.57
MAE (%)	IR	5.12	3.63	7.88	6.95	4.78	9.10
	NDFD	5.43	3.96	8.62	6.82	4.41	10.31
RMSE (%)	IR	7.09	4.70	10.11	9.05	6.22	11.27
	NDFD	7.50	5.53	10.33	9.50	6.25	12.79

IR CMV Forecasting Challenges

Cloud cover detection is a challenging task if only IR satellite data is available. The evaluated IR CMV forecast model relies on thresholding cloud top and ground temperatures to identify cloud cover. Lower altitude, warm clouds (i.e., marine layer stratus clouds) are the most challenging to detect due to the low temperature contrast between cloud top and ground.

The current IR CMV model challenge is illustrated in Figure 10. It suggests that the primary reason why IR CMV forecasts struggle at both BA and LA sites is due to warmer, marine layer clouds which frequently occur in these regions. Additional IR satellite cloud thresholding techniques are being evaluated that will help with the detection and subsequent CMV forecast of marine layer stratus clouds.
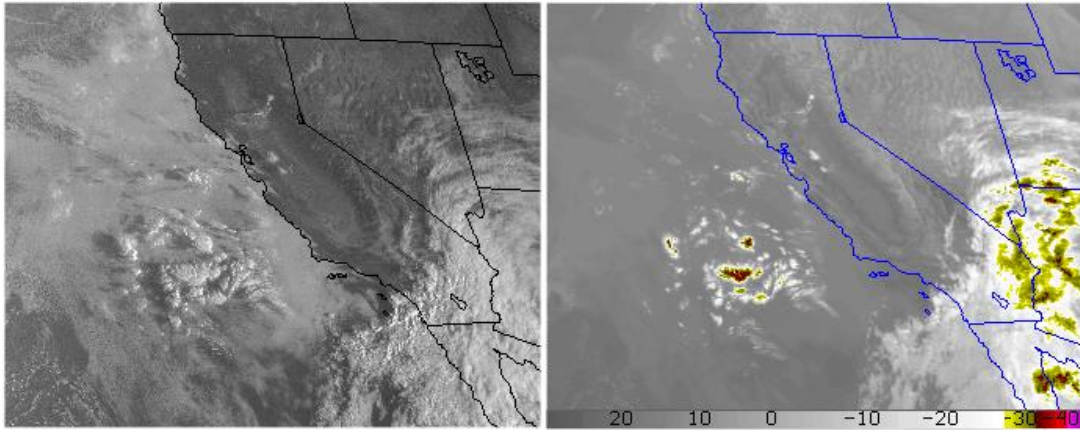
Figure 10: Example GOES visible (left) and infrared (IR) (right) satellite images from 10/7/2014 at 06:45 LST. The IR channel enhanced temperature (oC) scale is shown on the bottom of the IR image. Lower, warmer marine layer clouds are clearly observed in the visible GOES imagery but are hard to distinguish in the IR GOES imagery. Higher, colder clouds are better discernable in IR satellite images due to the thermal contrast present between the colder cloud tops and the warmer land surface.

Aside from the above challenges, day-to-day PV site availability and irradiance-to-power translation with reliable site specifications are also problematic. Decreased power production not related to changes in weather (e.g., inverter outages, PV module soiling, etc.) is not accounted in CMV and NWP forecasts, yet forecast validation is performed against real-life production data that tends to have varying availability. In addition, accurate PV site specifications (module type, inverter type, array configuration, etc.) are often challenging to obtain directly and have to be estimated at many PV power sites. These limitations make accurate irradiance-to-power translation difficult and often result in reducing the skills of CMV and NWP irradiance forecasts.

UCSD WRF and ODML Model Forecasting Results (Task 2 Highlights)

WRF and ODML forecasts and the associated effect on PV power production are evaluated at eight various sized PV plants located in four climate-specific locations in California as shown in Figure 11. Locations evaluated include the BA, LA, inland (D) and San Joaquin Valley (SJV). These eight PV plant locations represent the coastal, inland valley and desert climate regions of California, which compose forecast regions pertinent to the California ISO and are listed Table 3.
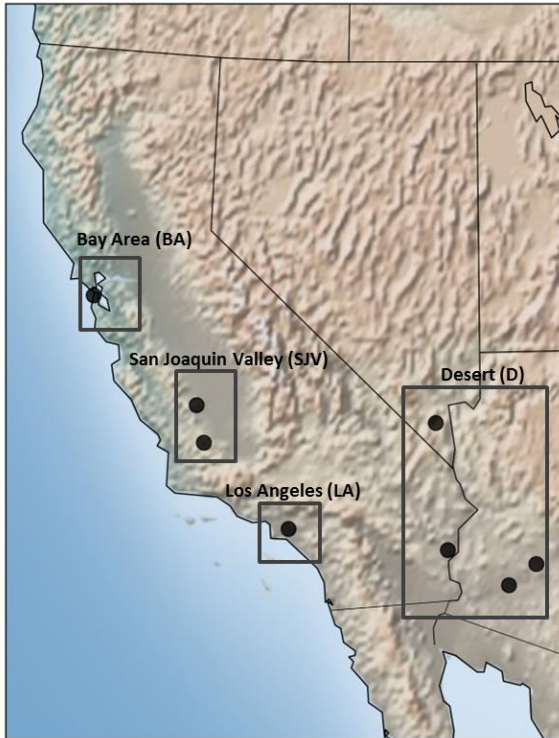
Table 3: Summary of PV plant locations and size.

PV site	Climate Region	PV plant Size
BA-1	Bay Area	Small
LA-1	Los Angeles	Small
SJV-1	San Joaquin Valley	Small
SJV-2	San Joaquin Valley	Large
D-1	Desert	Large
D-2	Desert	Small
D-3	Desert	Small
D-4	Desert	Large

Figure 11: PV solar plant forecasting locations (8) and climate zones (4) evaluated in this section.

Initial WRF-SolarCA Forecast Results

UCSD ran WRF-SolarCA forecasts initialized once a day (at 4:00 PM LST). Resulting forecasts were generated at 4 km horizontal spatial and 15-minute time resolution spanning out to a 54-hour time horizon. WRF model spatial coverage included all regions of interest to the California ISO. Error metrics performed on WRF-SolarCA and corresponding NDFD GHI forecasts at 8 various coastal and inland California PV sites determined that the WRF-SolarCA forecasts at all locations exhibited high error due to the under-prediction of clouds.

There are several reasons contributing to the initial poor WRF-SolarCA forecasting results. The most crucial one is a high clear sky bias present in the WRF-SolarCA forecasts, which results in high MBE and MAE metrics across all sites during all forecast horizon hours. This clear sky bias was determined to be due to the lack of realistic modeled atmospheric aerosols within the WRF model framework. Additionally, Mathiesen and Kleissl (2011) demonstrated that NWP models frequently under-predict cloud cover, resulting in further bias towards predicting clear skies.

DA WRF-SolarCA cloud forecasts lose all near-term forecast benefits gained from the cloud assimilation methods employed by UCSD are largely driven by the external grid NAM model forecasts which are notoriously poor at marine layer cloud forecasting

(Mathiesen and Kleissl, 2011). As a result of the forecast generation timeline, WRF-SolarCA forecasts exhibited an artificially high bias at the two coastal sites (BA and LA) during the DA morning hours. The WRF-SolarCA DA forecasts were determined to be less accurate than NDFD forecasts.

After helpful discussions with UCSD it was determined that these results were undesirable and that it would be worthwhile to refocus WRF-SolarCA forecasts onto a more appropriate forecasting effort. The results of the updated WRF-SolarCA forecasting efforts are presented below.

Updated WRF-SolarCA Forecast Results

WRF-SolarCA Model Overview and Setup

It was determined that WRF-SolarCA forecasting efforts should be focused on an applicable forecast need for this effort. The most promising effort was to improve upon marine stratus cloud forecasts in the coastal regions of California.

To facilitate this effort, two nested model domains cover the region of interest, at 8.1 km and 2.7 km resolutions for the outer and inner domains, respectively. Their locations and sizes are shown in Figure 12. Vertically, the domain spans 75 vertical levels, with 50 levels below 3 km to help resolve boundary layer cloud formation.

Two sets of initialization data were used in this modeling effort. The first set is initialized at 06 UTC, from the 00Z-initialized North American Mesoscale (NAM) forecasts (i.e., the 6th hour forecast of the 00 UTC-initialized NAM), and is denoted by 06-00N. The second set is initialized at 12 UTC, from the 12 UTC-initialized NAM forecasts (i.e., the 0th hour forecast of the 12 UTC-initialized NAM), and is denoted by 12-12N. 06 and 12 UTC correspond to 11 PM and 5 AM LST, respectively, in California. In both sets, the parent simulation is driven by NAM forecast output on the 218 AWIPS CONUS grid at 12-km resolution.
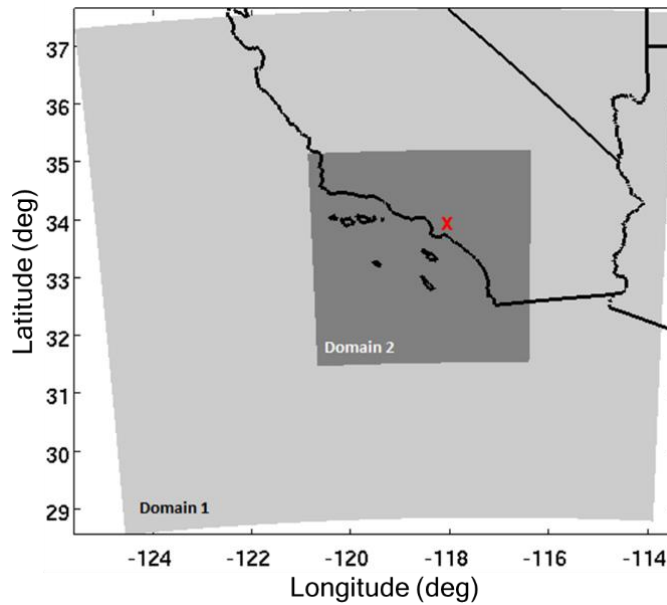
Figure 12: WRF-SolarCA domain configuration. Domain 1 is at 8.1 km resolution, while domain 2 is at 2.7 km resolution. Location of targeted LA Basin photovoltaic site (LA-1) is indicated by the red X.

Physics Parameterizations

A summary of physics parameterizations is given in Table 4. WRF version 3.6 was run during these simulations.

Table 4: Summary of WRF parameterization schemes

Parameterization type	WRF setting (Outer/inner domain)	Scheme name
Planetary boundary layer	5/5	MYNN2
Surface layer	5/5	MYNN
Land surface	2/2	Noah LSM
Radiation (LW & SW)	5/5 for both, at 5 min time step	New Goddard*
Microphysics	10/10	Morrison 2-mom
Cumulus	14/0, at 1 min time step	New SAS

*The New Goddard radiation scheme includes the Rayleigh scattering correction by Zhong and Kleissl (2015) that eliminates bias in Global Horizontal Irradiance.

Preprocessing Schemes Evaluated

CLDDA (CLouD Data Assimilation)

The Cloud Data Assimilation (CLDDA) package (Mathiesen, Collier, & Kleissl, 2013) is a preprocessing suite which alters the relative humidity fields in WRF in accordance to cloud positions as determined by satellite imagery.

In brief, the latitude and longitude positions of low clouds are determined from the GOES sounder cloud product maintained by CIMSS at the University of Wisconsin-

Madison. In cloudy columns, cloud tops are defined at the inversion base height or, in the absence of an inversion, at the intersection of the vertical temperature profile and satellite cloud-top temperature. Cloud base height is determined from an empirically-derived function relating cloud base height to cloud top height. Lastly, relative humidity is adjusted to 110% within the cloud deck and all previous liquid water is zeroed. In order to avoid excessive latent heating from the subsequent condensation, microphysics heating is turned off for 1 hour following application of CLDDA. Additionally, relative humidity is adjusted to a maximum of 75% in clear columns as determined by GOES imagery.

WEMPP (Well-Mixed PreProcessor)

Because liquid water content is not directly transferred from NAM to WRF, a "spin-up" period of approximately 6 hours is required for the microphysics scheme to regenerate a liquid cloud field from zero. In an effort to reduce this spin-up period, the Well-mixed Preprocessor (WEMPP) was developed in order to provide a better initial guess of cloud liquid water at initialization. The method is as follows:

1. In columns containing a temperature inversion under 3 km, the highest grid point under the inversion base height at relative humidity (RH) ≥ 95% is defined as cloud top.
2. Assuming a single cloud layer, mass-weighted averages of RH are computed downwards in layers of increasing depth until the layer average RH < 95%. The bottom-most point is defined as cloud base.
3. The water vapor mixing ratio q_v is set to the saturation water vapor mixing ratio q_{sat} at cloud base. Applying the well-mixed layer assumption, q_{sat} at cloud base is equivalent to the total water mixing ratio q_t (the sum of water vapor and liquid water mixing ratios $q_v + q_l$) within the boundary layer.
4. Within the cloud layer, q_v is set to q_{sat}, and the difference between q_{sat} and q_v is partitioned into q_l.

WEMPP and CLDDA are further combined into an ensemble known as Well-Mixed PreProcessor Data Assimilation (WEMPPDA). Further details on the WRF-WEMPPDA ensemble are described in Table 5.

IBH (Inversion Base Height)

A negative bias in WRF-simulated inversion base height (IBH) was determined from comparisons with observational data. Since marine stratus cloud layers are capped by a temperature inversion, low IBH can not only lead to decreased cloud thickness, but also restrict inland advancement of cloud cover in regions where land elevation exceeds the IBH.

Therefore, a preprocessing method was developed to raise all present non-surface temperature inversions under 3 km by a fixed height. After increasing the IBH, the mass-weighted average q_t is computed from the old planetary boundary layer (PBL) and applied to both the old and supplemental PBL. Following, q_v and q_l are partitioned as described in WEMPP methodology. The temperature within the former PBL remains unchanged, and the supplemental PBL temperature profile is set according to the dry or

saturated adiabatic lapse rate, for clear and cloudy conditions, respectively. Temperature and moisture within the inversion layer is simply shifted vertically in order to maintain inversion depth, strength, and gradients. An example of original and adjusted vertical profiles is shown in Figure 13.
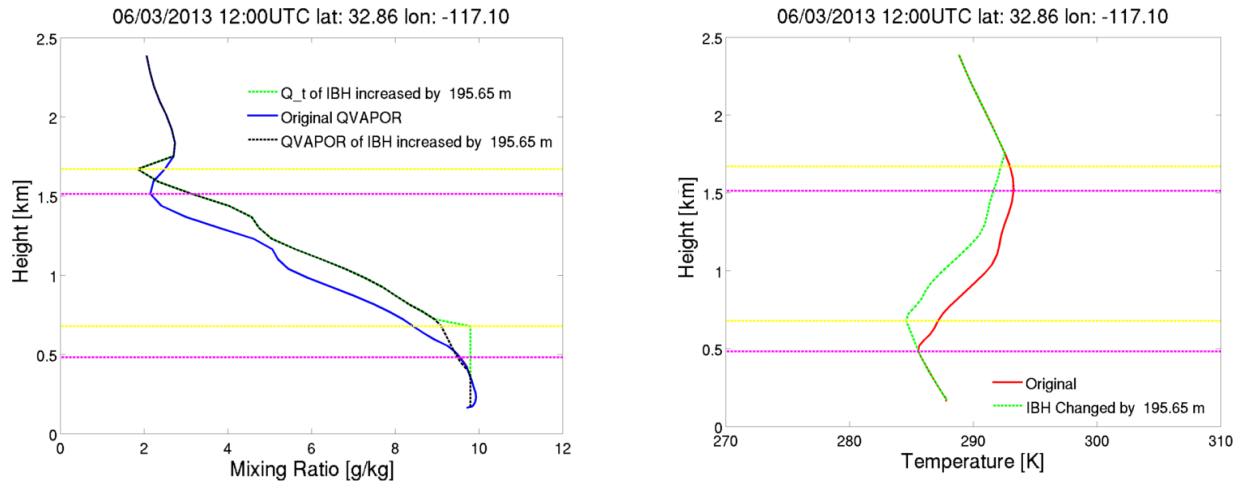

Figure 13: The original [adjusted] inversion layer is demarcated by dashed magenta [yellow] lines. Left: Computed total water mixing ratio (dashed green), and original [adjusted] water vapor mixing ratio in blue [dashed black]. Right: Temperature profiles in original PBL (red) and adjusted PBL (dashed green).

WRF-SolarCA Model Ensembles

A summary of WRF-SolarCA model forecast ensembles evaluated in this report is given in *Table 5*.

Table 5 - Summary of WRF-SolarCA ensembles

Name	WRF-WEMPPDA	WRF-IBH
Initialization	12-12N	06-00N
Preprocessing	WEMPP + CLDDA at initialization*	IBH adjustment at initialization**
Forecast horizon	42 hours	48 hours
Processing time (estimate based on 60 processors)	3.5 hours	4 hours

* This ensemble is the combination of two preprocessing schemes. In run 1, only WEMPP will be applied. In run 2, CLDDA will be applied at initialization. After one-time step, both simulations will be stopped. In each grid column, the moisture profile of the run with the greatest liquid water path will be set in run 2, and the simulation will resume.

** Adjustment will be equal to the average inversion bias at Miramar (KNKX) determined in June 2013 (300 m).

WRF-SolarCA Model Post-Processing

A simple MOS correction was applied based on clear sky index (model GHI normalized by clear sky GHI) and solar zenith angle. A rolling 30-day window is used to fit the MOS function to reduce clear sky WRF-SolarCA forecast bias errors.

WRF-SolarCA Model GHI Forecast Results

WRF-SolarCA GHI forecast error metrics are shown in figures 14-16 below at the LA PV site. Results are shown from June 23-26, 28-30; July 1-2; August 6-12; and September 4-5, 20-21 from 2014 which all represented days dominated by marine stratus cloud conditions. WRF-SolarCA ensembles included in the analysis are WRF-WEMPPDA and WRF-IBH. Irradiance forecast validation was performed against SolarAnywhere GHI data at 30-min 0.02° resolution and 24-hour persistence.
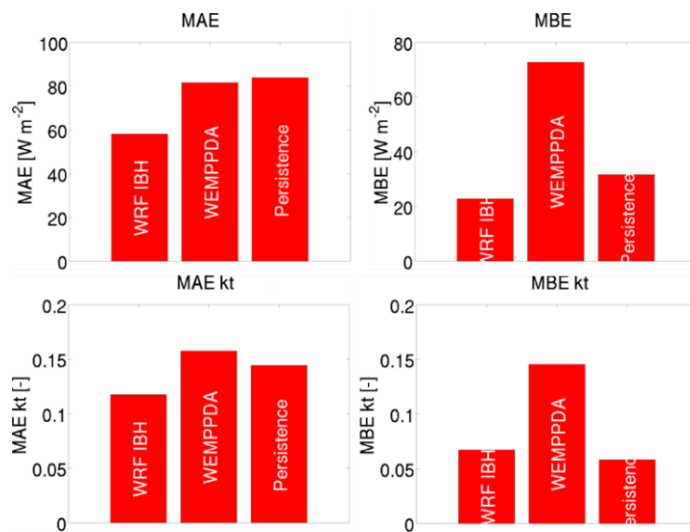

Figure 14: WRF-CA LA Basin site GHI error statistics.

*Figure 15: Zoomed spatial MBE kt error maps. Left: WRF-WEMPPDA. Right: WRF-IBH. Daily averages from 7:00 AM to 6:30 PM local time, averaged over all days. The Los Angeles region PV site location is denoted by the black X. *Note: Aug. 11 is excluded from these plots due to a post-processing error.*
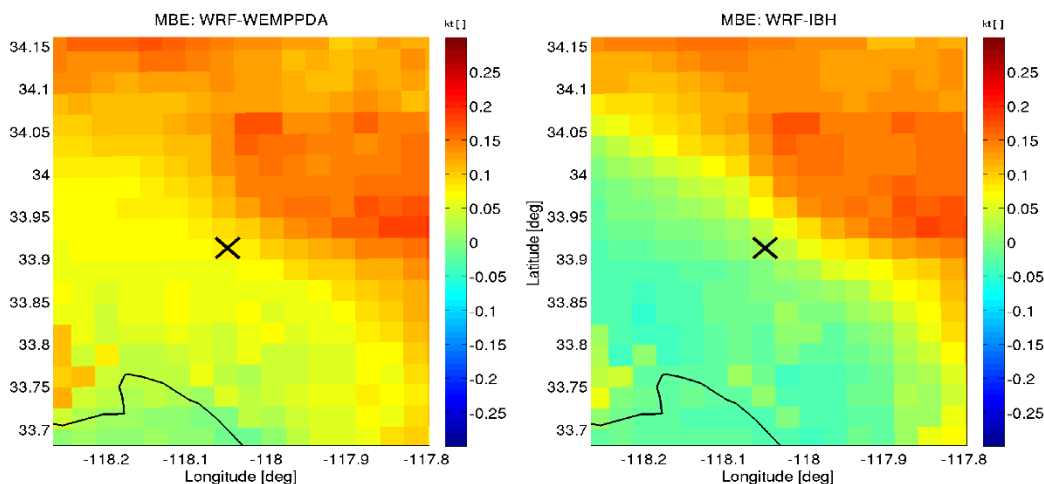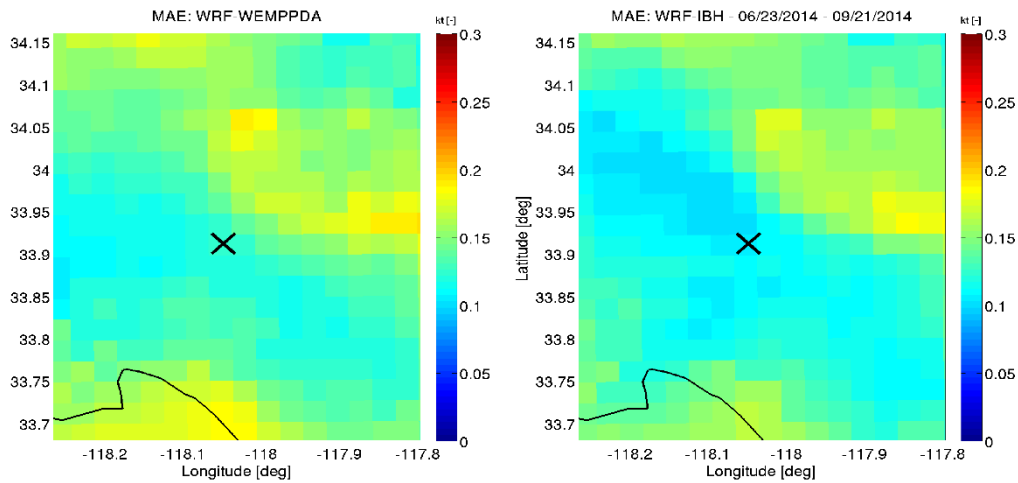
Figure 16: Zoomed spatial MAE kt error maps. Left: WRF-WEMPPDA. Right: WRF-IBH. Daily averages from 7:00 AM to 6:30 PM local time, averaged over all days. The Los Angeles region PV site location is denoted by the black X. *Note: Aug. 11 is excluded from these plots due to a post-processing error.

In conclusion, of the two ensembles evaluated in this update, WRF-IBH is the best performer, showing low bias error, even when compared against persistence forecast. WRF-IBH outperforms persistence forecast in every metric except MBE_{kt}. WRF-WEMPPDA exhibits a strong positive bias, suggesting failure to predict adequate cloud cover in the region.

WRF-SolarCA Model PV Energy Forecast Results

As part of Task 3 efforts WRF-SolarCA model irradiance forecasts were translated to PV power via the process described earlier in this report and compared to real-world observations of PV energy at the LA region PV site (LA-1) located on the west side of the LA Basin. A map of the LA region PV plant location is shown in Figure 17.
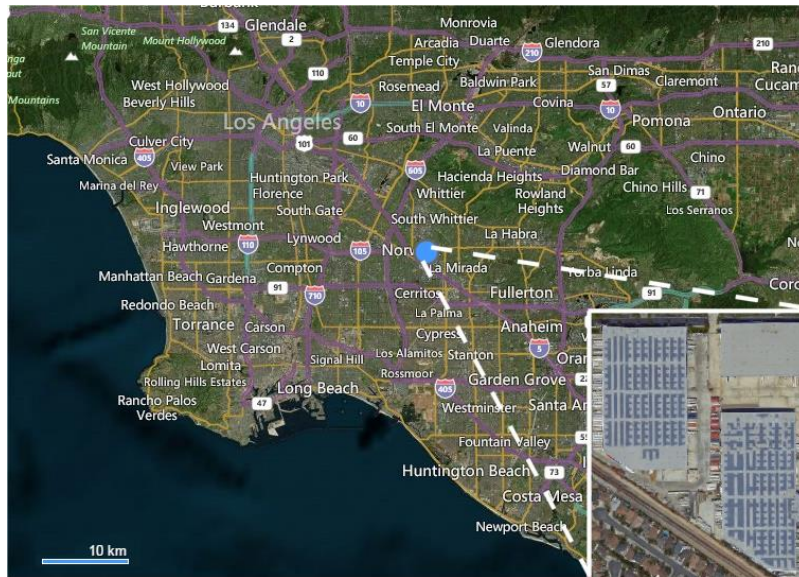
Figure 17: LA-1 PV plant location (denoted by the blue dot). A zoomed in view of the PV plant location is shown in the lower right inset. Map images courtesy of Bing Maps.

WRF-SolarCA PV power forecast error metrics are shown in Table 6 below at the LA-1 PV site. Results are shown from June 23-26, 28-30; July 1-2; August 6-12; and September 4-5, 20-21. WRF-SolarCA ensembles included in analysis are WRF-IBH and WRF-WEMPPDA. Validation was performed against hourly-averaged PV power plant data from the LA-1 PV site.

Table 6: Hourly PV error metrics at the LA-1 site. For MAE and RMSE, models with lowest error in each respective hour are shaded green, while models with highest error are shaded red.

LA-1 PV Site	Forecast Metric (MAE)			
Forecast Valid Time (LST)	WRF-IBH	WRF-WEMPPDA	IR CMV	NDFD
6	0.71%	0.95%	0.94%	1.07%
7	2.69%	3.62%	9.34%	4.40%
8	5.19%	10.55%	20.58%	5.74%
9	9.77%	14.59%	23.50%	17.68%
10	12.76%	15.34%	17.54%	18.57%
11	12.13%	13.07%	12.11%	11.49%
12	7.89%	9.62%	9.00%	7.72%
13	5.39%	5.91%	6.35%	5.54%
14	6.54%	6.74%	6.06%	6.22%
15	5.30%	5.38%	5.67%	5.57%
16	4.13%	4.13%	4.69%	4.56%

LA-1 PV Site	Forecast Metric (RMSE)			
Forecast Valid Time (LST)	WRF-IBH	WRF-WEMPPDA	IR CMV	NDFD
6	0.91%	1.18%	1.06%	1.25%
7	3.76%	4.98%	10.00%	5.27%
8	6.39%	12.10%	22.42%	7.61%
9	11.08%	17.36%	28.54%	22.62%
10	15.73%	21.46%	24.79%	25.88%
11	17.84%	21.21%	21.55%	21.58%
12	13.58%	17.44%	16.49%	15.97%
13	8.36%	8.69%	9.25%	8.78%
14	7.76%	7.96%	7.30%	7.88%
15	6.15%	6.24%	6.38%	6.51%
16	4.42%	4.48%	5.24%	5.00%

Once again, WRF-IBH is the best performer, showing consistently low bias error, particularly during morning hours. IR satellite-based CMV forecasts show high error during morning hours due to their challenges detecting marine stratus clouds, though modest improvement occurs in the afternoon. WRF-WEMPPDA and NDFD present mixed results, also showing high MBE in the morning. In conclusion, WRF-IBH is the most accurate of the 4 models at forecasting PV power generation at the LA Basin PV site during the 20-day marine layer cloud-focused intensive observation period.

ODML Model Overview and Background

Professor Carlos Coimbra's Lab at UCSD developed an Optimized Deep Machine Learning (ODML) forecast model that ingests CPR's PV irradiance and energy forecasts. The goal of this model is to reduce the ensembled forecast error to its irreducible level. This task is motivated by the fact CPR's PV forecasts are based on a combination of satellite-based and NWP irradiance forecast data as well as predicted weather, which are both known to contain data-to-irradiance limitations that can impact forecast accuracy.

The ODML model employs hierarchical, multi-layer learning features that are based on ensemble learning representations. These forecast engines combine the adaptive nature of hybrid Genetic Algorithm (GA) and Artificial Neural Networks (ANN) with dynamic input selection, and fractional pre-processing in a multi-layered algorithm that allows for several hierarchical representations in neural memory. The available data stream inputs are optimized using an advanced, predictive preprocessing methodology. These techniques are based on Professor Coimbra's Evolutionary Non-Integer Order (ENIO) pre-processing that determines relevancy and optimizes input selection to the forecasting engine. ANN topology is continuously and dynamically optimized using GAs that scan the solution space and "evolve" the ANN structure. This avoids time-consuming trial-and-error approaches that have limited chance to result in optimal ANN

topology. The ODML techniques are able to learn the errors resulting from inaccuracy specifications and adjust the forecasts accordingly. Figure 18 describes the workflow for the ODML model.
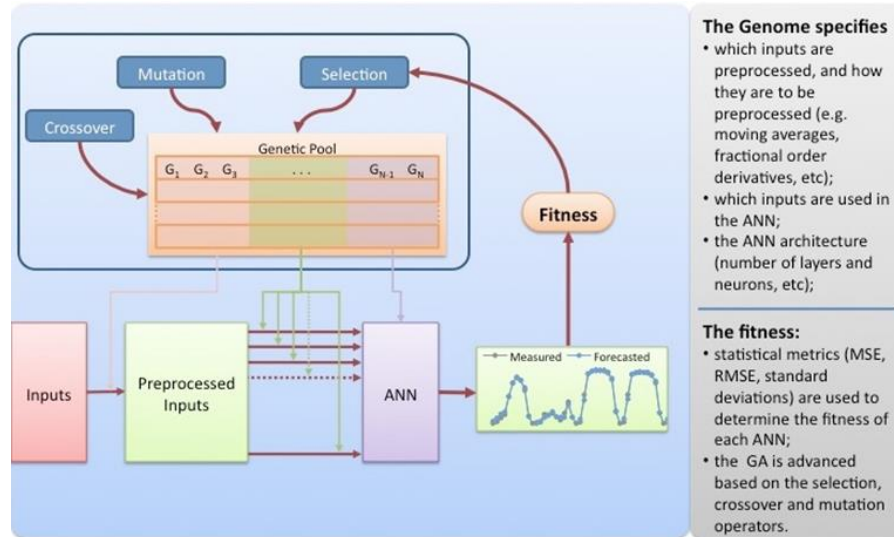

Figure 18 The Hybrid Evolutionary Non-Integer Order algorithm used to control the selection of Artificial Neural Networks in our Forecasting Methodology.

Genetic algorithms are biological metaphors that combine an artificial survival of the fittest with genetic operators abstracted from nature. In this optimization technique, the evolution starts with a population of individuals, each of which carrying a genotypic and a phenotypic content. The genotype encodes the primitive parameters that determine an individual layout in the population. In the adopted strategy the genotype consists in the binary weights (masks) that control the inclusion/exclusion of inputs from the ANN, and other parameters that control the preprocessing of input variables such as the order of the fractional order derivative, the window size for moving average preprocessing, etc. Additional parameters that control the ANN architecture, transfer functions, etc. can also be added to the individual genome. The GA optimizes these parameters by evolving an initial random population such that the RMSE between the historical data and forecasting data is minimized.

One of the key components in the ODML models is the use of non-integer derivatives (fixed or variable) to preprocess input data when needed. The fractional derivatives, which are based on an integro-differential operator, generalize the meaning of ordinary constant order derivatives. In the case of solar irradiation, the short- and long-term memory effects on ground irradiance caused by periodic cloud cover (and PV power plant output) can be more accurately captured by non-Markovian processes. By using fractional derivatives these memory effects are coded as simple non-integer orders as inputs for the preprocessing stages, which in turn optimize the processing of inputs for minimum translation errors.

The performance of the ODML forecast is assessed using universally accepted error metrics such as the MAE, RMSE and the forecast skill relative to a reference model, in this case the original CPR FleetView irradiance and PV energy forecasts.

ODML Model Forecast Results

Individual ODML Forecast Results

For each of the 8 locations shown in Figure 11 UCSD created four ODML re-forecast models. Each model uses different input data:

- Model 1: GHI and DNI forecasts
- Model 2: PO (PV Power) forecast
- Model 3: PO and GHI
- Model 4: PO, GHI and DNI forecasts

Given that the original PV Power (PO) forecasts are based on three different data sources: IR and visible CMV and NDFD forecasts, the four ODML models were trained separately for each forecast data source.

The original datasets that contain PO, GHI and DNI data from 2014-05-14 to 2015-05-30 were divided into two disjointed sets: the training set and the validation set. The training set was used to determine the several free parameters in the ODML models while the validation set was used to assess the performance of the new forecast in terms of the MBE, MAE and RMSE error metrics. The improvement of the ODML models relative to the original forecasts was computed as:

$$S_i = \left(1 - \frac{\text{RMSE}_{\text{Model i}}}{\text{RMSE}_{\text{orig.}}} \right) \times 100\%$$

Figure 19 and Figure 20 illustrate the results obtained by the ODML models for two of the SJV PV sites and two of the Desert PV sites, characterizing a large PV array and a small PV array for each respective region. The top rows in the figures compare the four models against the original forecast. The results show that often Model 1 performs worse (negative values of forecast improvement) than the original model even though it is trained against measured PO data. In general, Model 4 outperforms all other models (Models 2 to 4), which is expected since it uses all the relevant data available.

SJV-1 PV Site

SJV-2 PV Site

Figure 19 Forecast performance for two SJV PV sites. (Top) Comparison of the forecast performance between the original PO forecast and the four ODML models. Negative values indicate that the respective re-forecast model performs worse than the original. (Bottom) Scatter plots that compare the original forecast and Model 4 (the re-forecast model as indicated by the top figures) against the measured values.
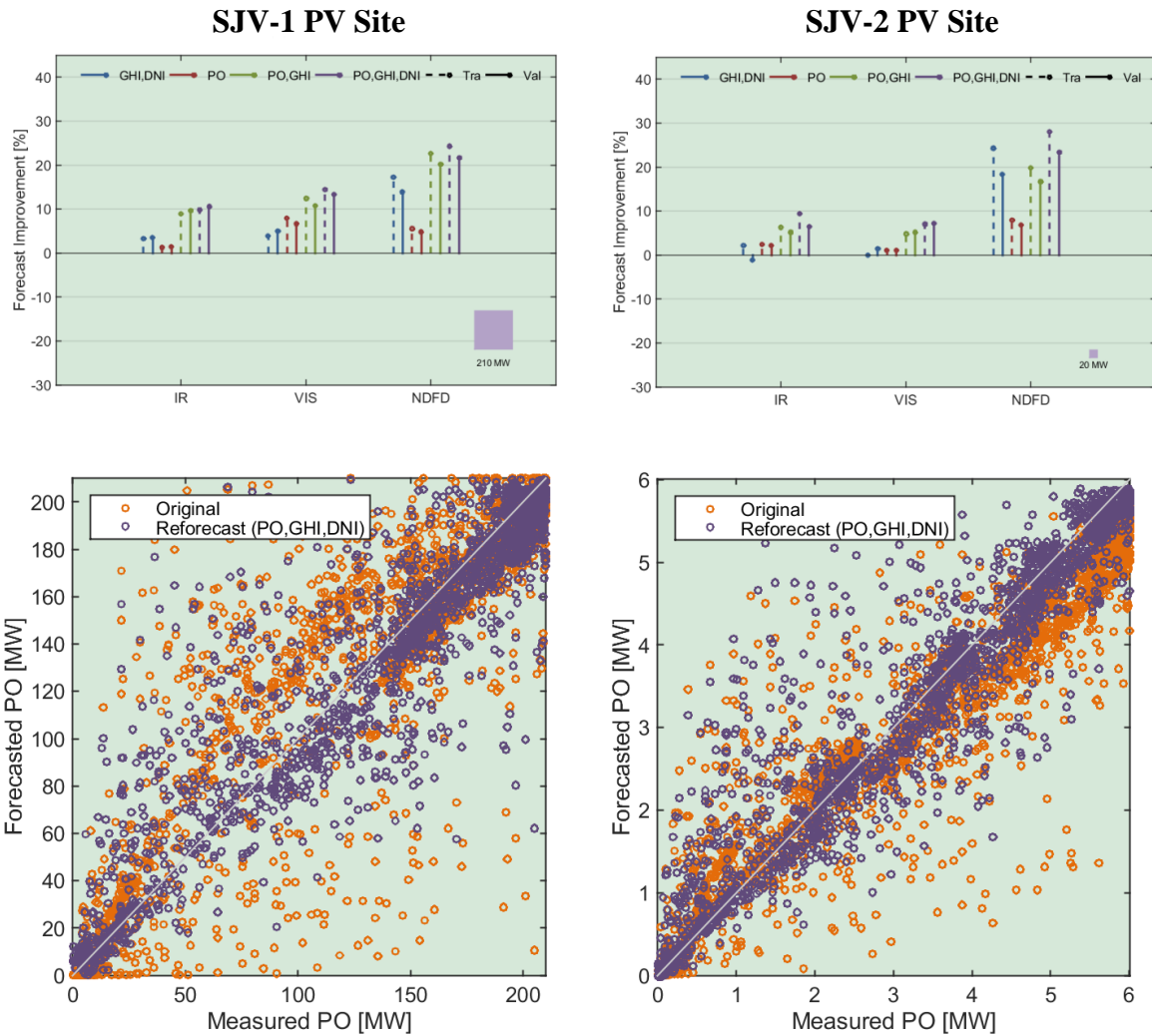
D-1 PV Site

D-2 PV Site

Figure 20 Forecast performance for two Desert region PV sites. (Top) Comparison of the forecast performance between the original PO forecast and the four ODML models. Negative values indicate that the respective re-forecast model performs worse than the original. (Bottom) Scatter plots that compare the original forecast and Model 4 (the re-forecast model as indicated by the top figures) against the measured values.
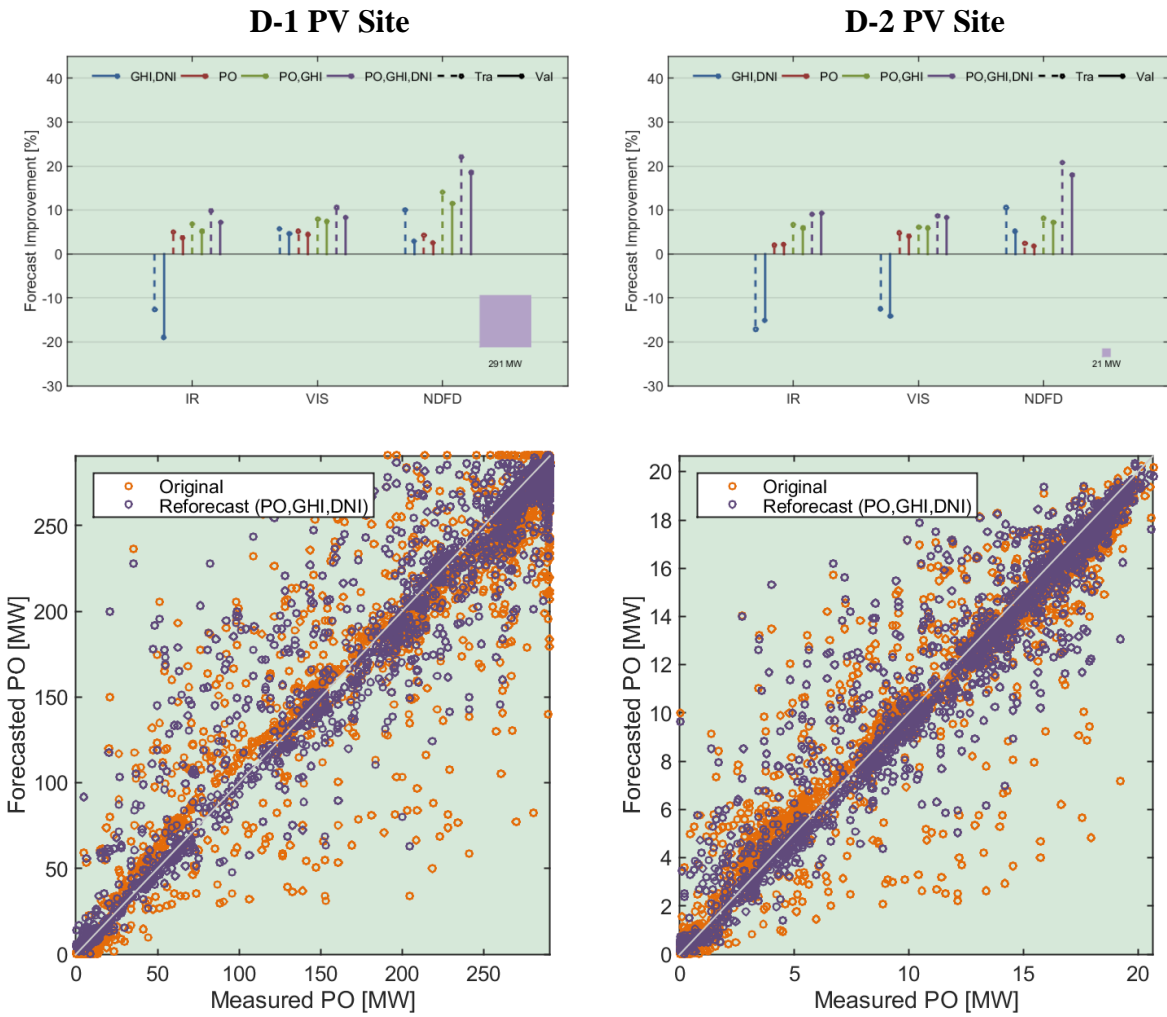
Finally, Table 7 reports error metrics for the validation set for the original PO forecast, the best ODML model (Model 4) and the worst ODML model (Model 1) for the 8 locations.

Table 7: Error metrics for individual forecast trained ODML models. Site prefixes denote location, as described in Table 3. Increased forecast error results are highlighted in orange.

	MBE			MAE			RMSE			Forecast improvement [%]	
	Orig.	Model1	Model4	Orig.	Model1	Model4	Orig.	Model1	Model4	Model1	Model4
Location:						BA-1 (small)					
IR	-0.29	0.01	0.01	0.58	0.55	0.51	0.80	0.69	0.65	13.65	18.72
VIS	0.11	0.02	0.01	0.45	0.43	0.41	0.59	0.57	0.55	4.19	7.77
NDFD	0.12	0.00	0.01	0.54	0.46	0.45	0.77	0.63	0.62	18.67	20.34
Location:						LA-1 (small)					
IR	-0.08	0.00	0.00	0.12	0.09	0.09	0.17	0.13	0.13	21.32	23.63
VIS	-0.02	0.00	0.00	0.12	0.08	0.08	0.16	0.12	0.11	25.71	29.90
NDFD	-0.05	0.00	0.00	0.13	0.09	0.08	0.19	0.13	0.13	30.90	33.58
Location:						SJV-1 (small)					
IR	-0.45	0.04	0.01	1.53	1.72	1.43	2.54	2.56	2.36	-0.83	6.80
VIS	-0.06	-0.03	-0.03	1.64	1.72	1.47	2.50	2.48	2.34	0.76	6.58
NDFD	-0.56	-0.01	-0.03	1.65	1.44	1.29	2.79	2.28	2.14	18.41	23.36
Location:						SJV-2 (large)					
IR	4.93	1.22	1.34	22.22	20.34	17.68	31.19	29.95	27.81	3.97	10.83
VIS	8.89	-0.74	-0.30	21.08	18.66	15.72	28.23	26.81	24.45	5.03	13.37
NDFD	0.97	0.84	1.06	20.32	17.61	15.36	31.73	27.29	24.85	13.99	21.67
Location:						D-1 (large)					
IR	4.85	0.21	0.09	21.14	27.52	17.59	33.79	40.15	31.36	-18.83	7.20
VIS	7.68	0.25	-0.24	22.86	20.19	17.63	34.08	32.57	31.34	4.45	8.06
NDFD	4.62	0.13	-0.84	19.43	20.51	14.94	33.02	32.06	26.92	2.91	18.49
Location:						D-2 (small)					
IR	0.37	0.05	0.04	1.42	1.75	1.14	2.24	2.58	2.04	-14.97	9.22
VIS	0.55	0.08	0.10	1.39	1.60	1.08	2.02	2.31	1.85	-14.09	8.41
NDFD	0.20	0.03	0.04	1.21	1.25	0.99	2.08	1.97	1.71	5.21	17.99
Location:						D-3 (small)					
IR	-1.34	0.11	0.05	3.80	5.63	3.86	6.70	7.71	6.12	-15.00	8.71
VIS	-1.72	0.05	0.07	3.47	4.72	3.52	6.12	6.72	5.65	-9.75	7.60
NDFD	-0.69	-0.01	0.05	3.67	4.15	3.17	6.20	6.22	5.27	-0.34	14.97
Location:						D-4 (large)					
IR	-0.86	0.34	-0.24	13.53	15.18	11.63	20.50	22.29	18.89	-8.71	7.90
VIS	1.81	0.06	0.01	13.17	12.90	11.55	19.54	19.23	18.11	1.56	7.28
NDFD	0.79	0.49	0.16	14.28	11.71	10.82	23.42	18.35	17.91	21.63	23.51

For the individual ODML forecasts, Model 4 (with GHI, DNI, and PO inputs) allowed for the greatest overall improvement. This is not surprising, as ODML output generally improves in accuracy with the addition of relevant inputs. NDFD forecasts had the most significant and consistent improvement when run through ODML, with IR and visible CMV forecasts varying from mild to significant improvement (Model 4) to an outright decrease in accuracy in some cases (Model 1). Coastal PV sites (BA-1 and LA-1) showed the greatest improvement in individual trials likely due to the ODML forecast corrections associated with marine layer cloud formation and dissipation.

Ensemble ODML Forecast Results

The most promising aspect of the ODML process is the creation of an ensemble PV forecast. Ensemble ODML forecast were created using the same inputs (IR and visible CMV, NDFD), but with all three inputs under the same configuration. For each one of the 8 selected locations we created four ODML re-forecast models for two forecasting cycles: the 7 AM LST and the 10 AM LST forecast times. Each model uses different input data:

- Model 1: GHI and DNI forecasts
- Model 2: Power (PO) forecast
- Model 3: PO and GHI
- Model 4: PO, GHI and DNI forecasts

The models for the 7 AM LST re-forecast uses CPR's forecasted data (PO, GHI and DNI) issued at 7 AM LST composed of IR CMV and NDFD forecast data. The re-forecast models for the 10 AM LST cycle use forecast data issued at 10 AM LST based in the IR and visible CMV, and NDFD forecast data.

The training data has been divided into two disjointed sets as discussed in the section above. The training set was used to determine the several free parameters in the ODML models while the validation set was used to assess the performance of the new forecast in terms of the MBE, MAE and RMSE error metrics. The results show that Model 4 ensemble forecast outperforms all other model forecasts (as shown in Table 8).

Table 8 Error metrics for the original forecast and the ODML re-forecasts and the improvement of the ODML re-forecasts relative to the two original forecasts. These error metrics were computed using the validation data set. MBE, MAE and RMSE values in MW. Site prefixes denote location, as described in Table 3.

	MBE			MAE			RMSE			Forecast improvement [%]	
	Orig.	Model1	Model4	Orig.	Model1	Model4	Orig.	Model1	Model4	Model1	Model4
BA-1 (small)											
7:00 AM	-0.317	-0.015	-0.012	0.632	0.451	0.437	0.843	0.612	0.594	27.445	29.57
10:00 AM	0.144	0.003	-0.006	0.478	0.438	0.439	0.622	0.582	0.576	6.441	7.38
LA-1 (small)											
7:00 AM	-0.08	-0.002	0.001	0.125	0.097	0.097	0.174	0.136	0.135	21.756	22.39
10:00 AM	-0.018	-0.001	0	0.129	0.08	0.078	0.175	0.116	0.112	33.808	36.186
SJV-1 (small)											
7:00 AM	-0.028	-0.07	-0.006	1.62	1.592	1.316	2.513	2.403	2.209	4.391	12.09
10:00 AM	-0.002	0.031	0.044	1.648	1.478	1.351	2.584	2.25	2.168	12.919	16.128
SJV-2 (large)											
7:00 AM	11.043	2.016	2.221	25.361	18.371	15.724	34.156	26.965	24.649	21.053	27.834
10:00 AM	10.552	0.182	0.293	20.656	15.567	13.779	27.887	22.763	21.839	18.375	21.686
D-1 (large)											
7:00 AM	9.472	-2.272	-1.666	23.896	18.65	12.808	34.609	29.873	24.387	13.686	29.537
10:00 AM	11.738	1.17	0.603	23.537	17.581	14.505	34.228	28.118	26.346	17.851	23.027
D-2 (small)											
7:00 AM	0.921	-0.003	0.009	1.736	1.254	0.916	2.62	1.89	1.579	27.84	39.719
10:00 AM	0.751	0.086	0.155	1.481	1.274	0.984	2.103	1.991	1.74	5.328	17.252
D-3 (small)											
7:00 AM	0.223	0.013	0.011	4.083	4.349	2.995	6.54	6.221	4.995	4.876	23.627
10:00 AM	-1.605	0.185	0.254	3.429	4.184	3.467	6.353	6.066	5.477	4.519	13.784
D-4 (large)											
7:00 AM	1.665	0.139	0.006	14.59	11.244	9.496	21.034	16.484	15.083	21.634	28.291
10:00 AM	2.467	-0.39	0.144	13.08	11.564	11.715	20.231	18.411	18.491	8.997	8.601

For both individual and ensemble ODML forecasts, Model 4 (with GHI, DNI, and PO inputs) allowed for the greatest improvement. In individual trials, coastal PV sites (BA-1 and LA-1) showed the greatest improvement, likely due to the influence of marine layer cloud formation and dissipation on input forecasts, while Desert PV forecasts showed moderate forecast improvement with all models. However, this trend was not obvious with ensemble forecasts. Additionally, PV array size does not appear to be a major factor in forecast improvement.

California ISO BTM Solar Load Forecast Results (Task 4 Highlights)

California Electrical Grid Background

The amount of electric power required at any specific time on an electrical system is known as the load. The demand for load originates with the energy-consuming equipment of the consumer. The California ISO is responsible for maintaining reliability and accessibility to one of the largest and most modern power grids in the world. The California ISO team works diligently 24 hours every day to "keep the lights on" while

meeting the electricity load needs of Californians through a competitive market-type supply and demand system. A map of the primary California ISO load balancing zones and sample daily load profiles are shown in Figure 21.
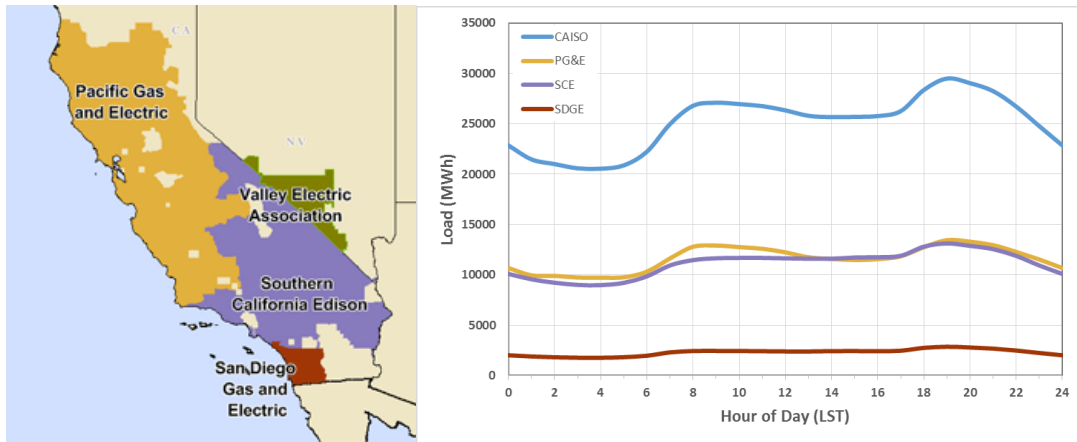

Figure 21: A map of California ISO load zones (left) and sample daily load profiles (right) from the three large investor owned utilities located in California on 1/22/2015 (publically available data obtained from www.oasis.caiso.com).

California ISO Automated Load Forecasting System (ALFS)

The California ISO operates an Automated Load Forecast System (ALFS) to generate short-term demand forecasts for California ISO Balancing Authority Area (BAA) operations. Supplied by Itron, ALFS utilizes an artificial neural network methodology that incorporates forecasted weather, such as minimum and maximum temperature, and conditions including type of day and business hour to determine the California ISO forecast of regional electricity demand. The system "learns" how to improve its load forecasting accuracy with increased experience based on historical observations.

The California ISO currently predicts load demand for five regional zones:

- PG&E Bay Area
- PG&E Non Bay Area
- SCE Coastal
- SCE Inland
- SDG&E

The two PG&E and SCE zones are sub-zones of the California ISO zones mapped in Figure 21. These zonal load forecasts are summed by California ISO to obtain a region-wide BAA load forecast. California ISO ALFS forecasts evaluated in this report include the three major load zones as shown in Figure 21.

FleetView Behind-the-meter (BTM) PV Historical Simulation and Forecasting Methodology

To date, CPR has worked with California ISO to collect all PV system information within the state of California. This list includes all BTM systems as well as large utility plants

and consists of PV system location, hardware capacity rating, installation angle specifications and shading (where available). The systems are also tracked by commissioning date so that historical simulations of total PV fleet output will provide an accurate representation of overall PV fleet performance history. Subgroups of BTM PV systems within the total fleet have been created based on California ISO designation. FleetView software was then tasked to simulate historical energy production for the five designated BTM PV fleets within California. An overview of the FleetView simulation methodology is shown in Figure 22. Each PV system is uniquely characterized and then simulated with the resulting power production summed into the aggregated PV energy from specified zones. Historical PV simulations are fed with SolarAnywhere satellite-based irradiance and weather data while forecasts are fed with a combination of CMV and NWP-based irradiance forecasts.
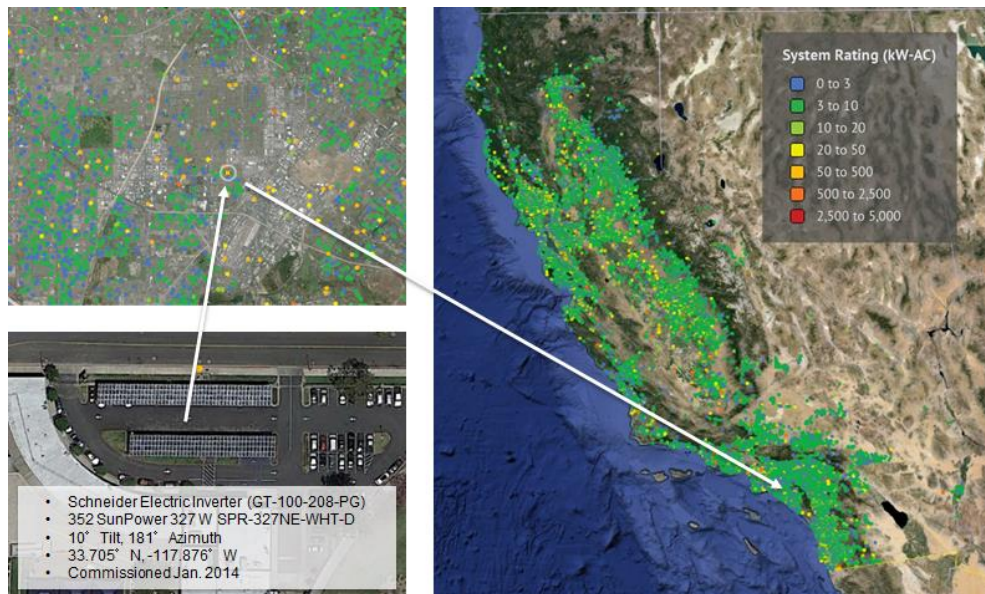

Figure 22: BTM FleetView simulation methodology where each PV system is located, characterized and simulated. Individual forecasts are aggregated into desired groupings and reported.

ALFS Historical Training Methodology and Statistical Results

California ISO and Itron conducted historical ALFS training incorporating historical load and BTM PV simulations from Jan 2010 to Feb 2014 as training input into California ISO's ALFS. An example of the historical BTM PV energy simulation and capacity are shown in Figure 23 for the PG&E zone. Zonal BTM PV capacity continues to increase over time as more BTM installed solar systems came online. Correspondingly, the zonal PV energy production also increases over time contributing to increasing offsets of corresponding consumer load.
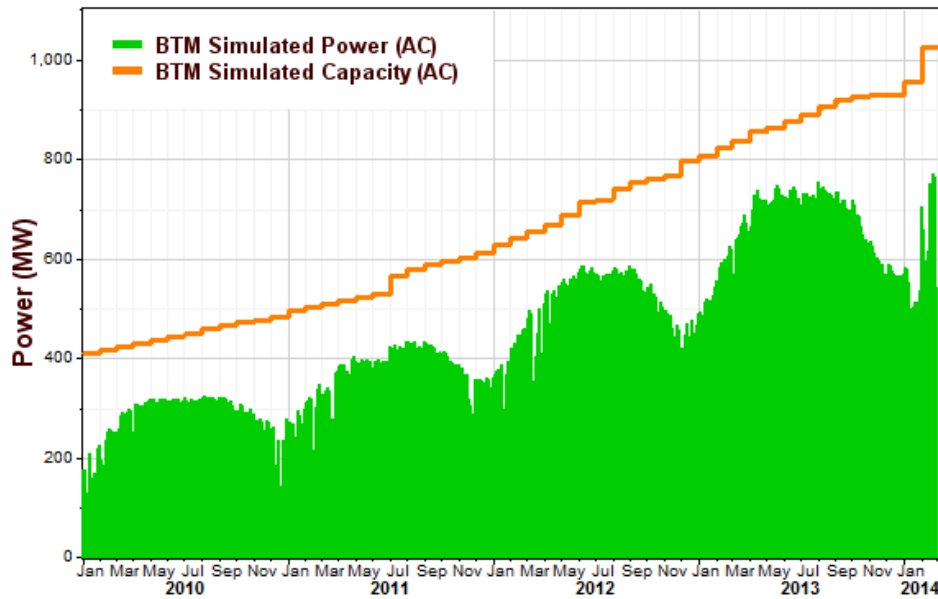
Figure 23: BTM simulated power (hourly) and capacity (monthly) from Jan 2010 to Feb 2014 for the PG&E load zone.

Results of ALFS historical training are shown in Table 9. Load forecasting error is observed to decrease at all hours of the DA forecast time frame when training includes historical BTM PV production. An ideal BTM coefficient of -1 indicates that for every predicted MW of BTM generation, one MW of load is shed. In other words, a BTM coefficient close to -1 would be the ideal scenario indicating that inclusion of the BTM PV forecasts in the ALFS training set is strategic. Table 9 also shows a statistically significant reduction in forecast error during mid-day and late-afternoon load forecasting periods. However, due to higher morning load variability and to the lower solar generation in the early morning hours, BTM production only offers a small impact for morning load forecasting.

Table 9: PG&E load zone DA ALFS historical training results.

Hour of Day-Ahead Forecast	9 am		12 pm		3 pm	
CPR BTM Dataset?	No	Yes	No	Yes	No	Yes
Load Forecast Error (MW)	122.3	121.7	136.7	130.1	149.3	142.7
Load Forecast Error (%)	1.11%	1.10%	1.18%	1.12%	1.27%	1.21%
BTM Coefficient	-	-0.21	-	**-0.92**	-	**-0.94**
T-test (significant if < -1.64)	-	-1.8	-	-10.1	-	-8.9

BTM-infused ALFS Forecast Performance

Forecast Horizons and Period Analyzed

Hourly resolution DA ALFS forecast data from 1/10/2015 to 9/15/2015, and hourly 30 minute-ahead data from 6/22/2015 to 9/15/2015, are compared against actual load data. Missing data have been excluded from the comparison. California ISO kindly supplied archives of hourly DA ALFS forecasts for the PG&E load zone along with 30 minute-ahead ALFS forecasts from the PG&E, SCE and SDG&E load zones. In all, 231 days of DA and 84 days of 30 minute-ahead ALFS regional load forecasts with and without BTM treatment are evaluated in this analysis.

DA Forecasting Error Metrics by Time of Day

DA ALFS forecast performance with and without the inclusion of BTM PV forecasts under all sky conditions are analyzed as a function of time of day in the PG&E load zone. Forecast error metrics by time of day are reported in bar graph form in Figure 24. An increase in forecast MAE and RMSE is observed during most hours when ALFS is run with input BTM PV forecasts, though improvements in MBE are noted in the morning hours. Time of day ALFS forecasting error results for the PG&E load zone under cloudy skies can be seen in Figure 25.
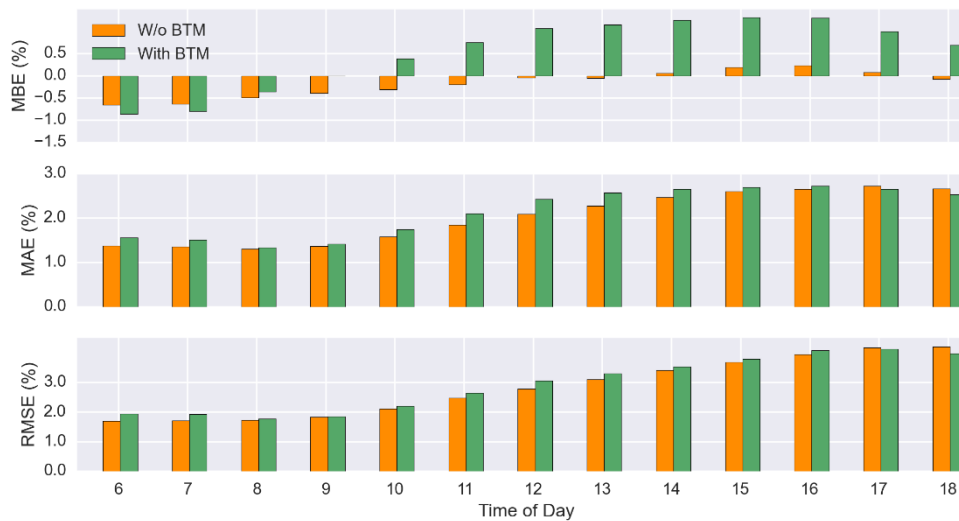

Figure 24: Hourly-averaged PG&E load zone DA ALFS forecast MBE, MAE and RMSE with and without BTM forecasts for the nine-month analysis period under all sky conditions.
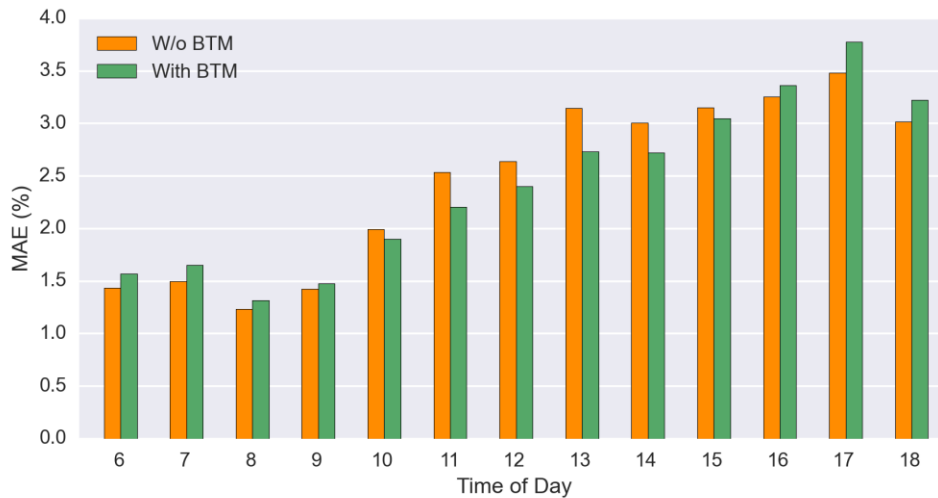
Figure 25: Hourly-averaged PG&E DA ALFS forecast MAE with and without BTM forecasts (cloudy hours).

Reduction in ALFS forecast MAE is noted during the majority of daytime hours for cloudy sky conditions when BTM PV data is included. The largest ALFS load forecast improvements are noted during peak daylight hours with a >15% reduction recorded at 1 PM. For clear sky conditions, forecast MAE reductions are significantly less, and in most cases MAE increases. While greater MAE improvements in the afternoon are observed during cloudy sky conditions, this is not the case for clear sky conditions. In fact, the afternoon ALFS forecast errors are larger with BTM treatment under clear sky conditions. Further investigation is needed to determine why ALFS responds this way with the inclusion of PG&E zone clear sky BTM PV forecasts.

30 Minute-Ahead Forecasting Error Metrics by Time of Day

30 minute-ahead ALFS forecast performance with and without the inclusion of BTM PV forecasts for the SDG&E zone under all sky conditions are analyzed as a function of time of day in Figure 26. SDG&E forecasts under all sky conditions demonstrate reduced error during traditionally less predictable morning hours when BTM forecasts are included as shown in Figure 27, respectively. Additionally, during cloudy sky conditions MAE is reduced during nearly all daylight hours.
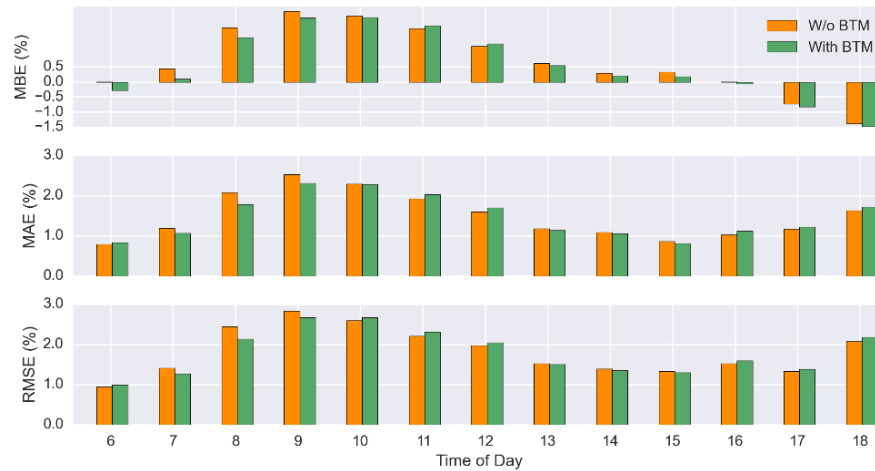
Figure 26: Hourly-averaged SDG&E 30 minute ahead forecast MBE, MAE and RMSE with and without BTM forecasts under all sky conditions.
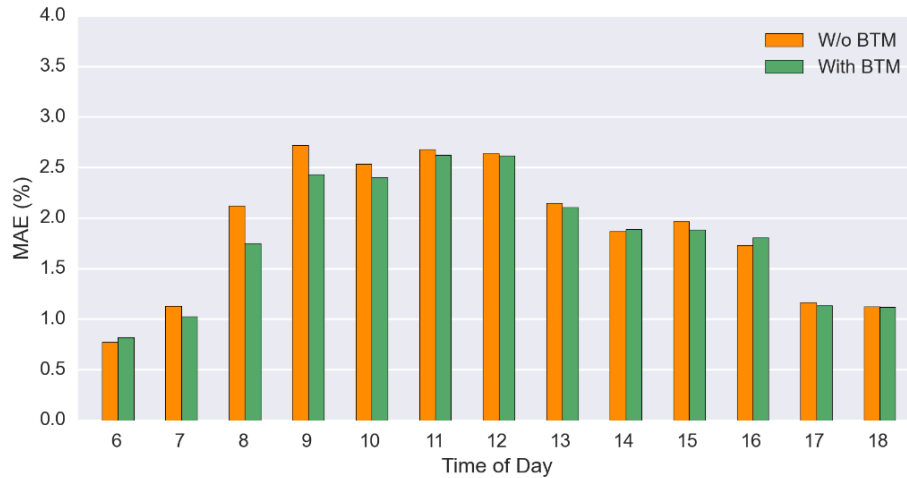

Figure 27: Hourly-averaged SDG&E ALFS 30 minute-ahead forecast MAE with and without BTM forecasts (cloudy hours).
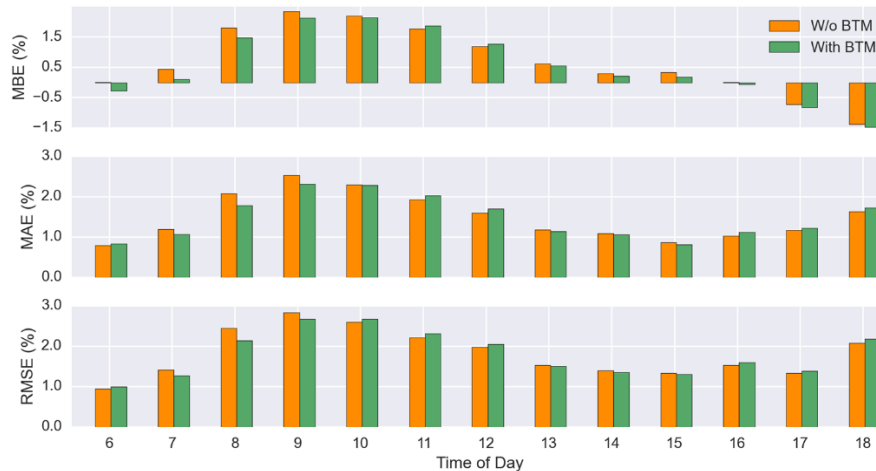
Figure 28: Hourly-averaged SCE ALFS 30 minute ahead forecast MBE, MAE and RMSE with and without BTM forecasts under all sky conditions.

When BTM forecast data are included, SCE 30 minute-ahead forecasts (Figure 28) also show reduced MBE, MAE, and RMSE during morning hours, but minor to negligible reductions elsewhere under all sky conditions. PG&E forecasts (not shown) demonstrated negligible or increased ALFS forecast error with the inclusion of BTM data throughout the day. The stronger impact of BTM PV data on SDG&E forecasts can be attributed to the geographic distribution of the utilities' respective load zones. Compared to SCE and PG&E, the load zone of SDG&E is relatively small and climatologically homogeneous, allowing for less regional variance in the forecasting results. Partitioning of SCE and PG&E load zones into the sub-zonal load regions described earlier – respectively PG&E Bay Area, PG&E Non Bay Area, SCE Coastal, and SCE Inland – could allow for similar forecasting accuracy improvements.

PG&E DA ALFS Error Metrics by Daily Clearness Index

Further insight into time of day ALFS forecasting error is gained when the analysis is distilled down into clear and cloudy hours. The Clearness Index (Kt) is incorporated in the study as defined in the following equation:

$$Kt = \frac{GHI_O}{GHI_{CS}}$$

where GHI_O is observed and GHI_{CS} is clear sky global horizontal irradiance. Clear sky conditions are noted when $Kt \geq 0.8$, and cloudy conditions are defined when $Kt < 0.8$. A Kt of 1.0 corresponds to a clear day while a Kt of 0.2 corresponds to a very cloudy day. During the time period from 1/10/2015 to 9/15/2015, daily Kt was calculated based on SolarAnywhere daily average GHI and SolarAnywhere daily average clear sky GHI. A clear day is defined when daily $Kt \geq 0.8$, and a cloudy day is defined when daily $Kt < 0.8$. Figure 29 shows a scatter plot of BTM included ALFS forecast MAE versus daily Kt. 71 of the observed days are classified as cloudy. We see that there was improvement on the daily level during a majority of clear and cloudy days.
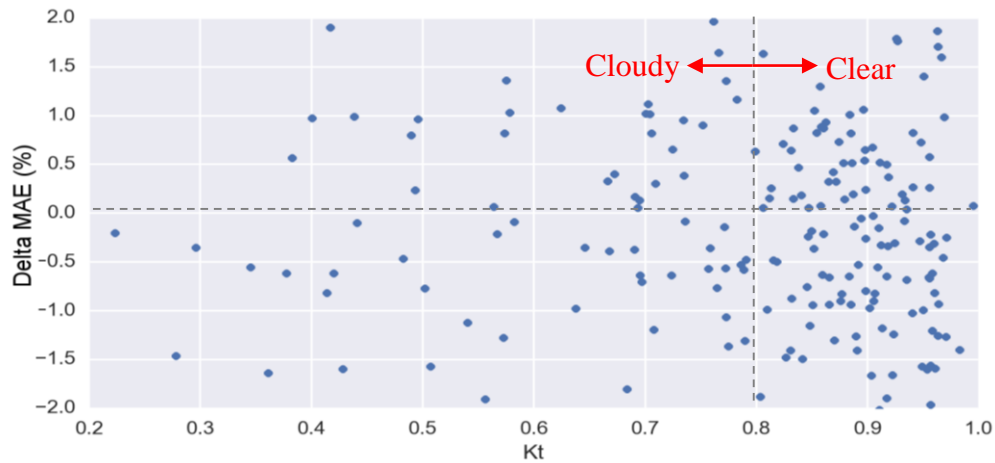
***Figure 29: Daily ALFS forecast delta MAE with BTM forecast treatment
(over non-BTM ALFS forecasts) binned by clearness index (Kt).***

Case Study: Five Cloudy Days in February

ALFS forecasting results for a five-day period of consecutively cloudy days during
February 2015 are reported here. Figure 30 shows GOES-West satellite imagery at
noon LST from Feb 5th 2015 through Feb 9th 2015. A large part of California is covered
by clouds and precipitation associated with an upper-level low pressure system located
offshore. This represents a challenging load forecasting period due to widely varying
cloud cover and temperature conditions associated with the passage of the upper level
low pressure system. Energy production from utility-scale and BTM PV fleet was
observed to vary significantly during this time period.

Figure 31 shows five days of ALFS DA load forecasts with and without the inclusion of BTM forecasts. Significant forecast improvements are observed during all daytime hours of the five-day period peaking with a nearly 50% reduction in load forecast error during the midday period of Feb 7th.
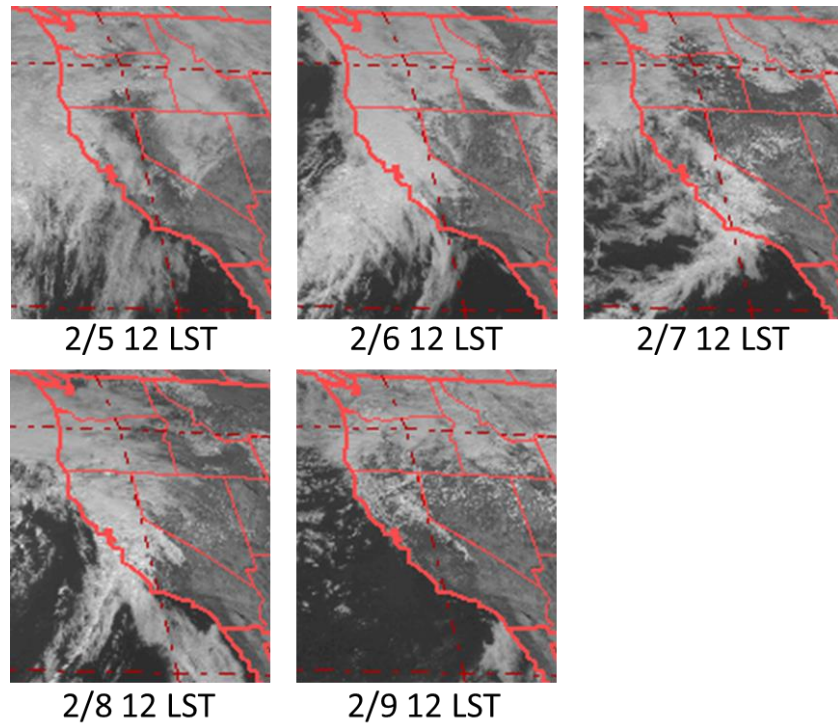

Figure 30: Daily 1200 Local Standard Time (LST) GOES-West visible satellite images spanning 2/5/2015 through 2/9/2015.
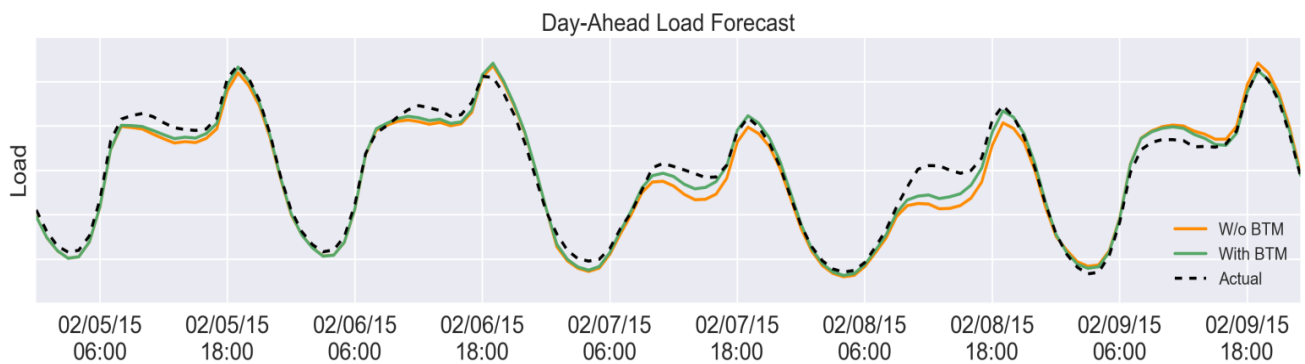

Figure 31: A five-day hourly time series of ALFS forecasts with and without BTM forecast versus actual load. Note that ALFS forecasts with BTM treatment are closer to the actual load during the daytime.

Tasks 5 & 6 (Public Data Access and Dissemination of Project Results)

CPR delivered a web-based interface to show a visual representation of the data collected. The site is publically available at: http://www.cleanpower.com/forecast-caiso/
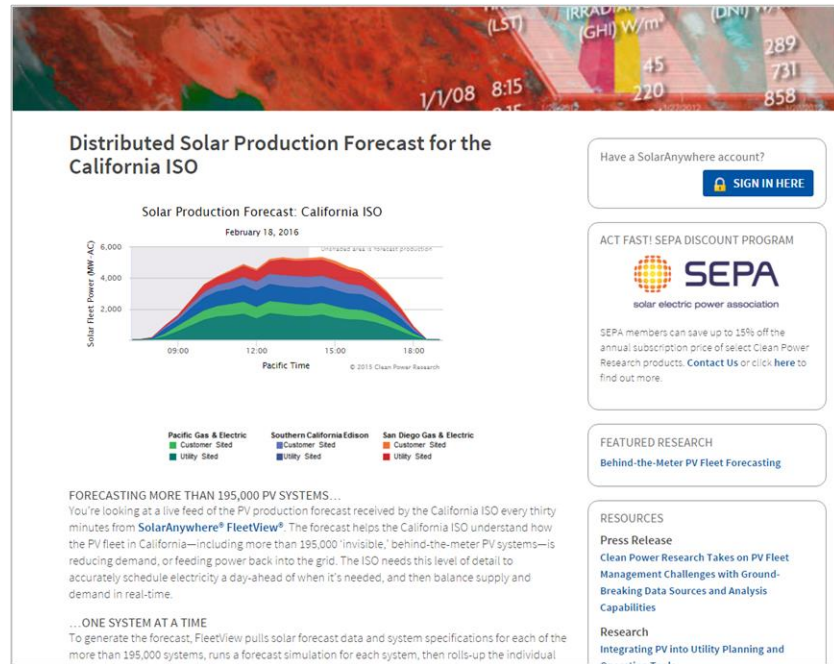

Figure 32:Screenshot of web portal that gives access to the forecast data referenced in this project.

Other activities that disseminate the findings from this project consist of technical presentations and conference publications. Such efforts are noted below.

- A New Operational Solar Resource Forecast Model Service for PV Fleet Simulation. Paper No. 44 – Presented at the IEEE PVSC 2014 held in Denver, CO (June, 2014).
- Distributed PV Simulation and Forecasting Experiences in California – Presented at UVIG Forecasting Workshop held in Denver, CO (February, 2015).
- Behind-the-Meter PV Fleet Forecasts Impacts on California ISO Load Forecasts – Presented as podium presentation at California utility forecasting workshop held in Folsom, CA (April, 2015).
- Integration of Behind-the-Meter PV Fleet Forecasts into Utility Grid System Operations – Presented as podium presentation at Third International Conference on Energy & Meteorology (ICEM) held in Boulder, CO (June, 2015).
- An update briefing on CPR's DOE Sunrise-sponsored work was presented to the California ISO onsite on Mon, Oct 5, 2015 1:00 PM.

Conclusions

Four major forecast research objectives were completed over the course of this study. Three new solar irradiance forecasting methods were examined and improved upon: The IR satellite-based CMV model; the WRF-SolarCA model and variants; and the ODML-training model and variants. These three forecasting methods were compared with existing methods such as NDFD and visible satellite CMV forecasts; and with operational PV plant power production allowing for real world applicable forecast metric evaluations. Additionally, an investigation was conducted on BTM fleet PV forecast impacts on the accuracy of California ISO load forecasts.

PV solar power forecast accuracy for the IR CMV model was evaluated through various error metrics at two specific sites in the San Joaquin Valley and LA regions, along with aggregate forecast error results evaluated for three California climate regions which were composed of 32 utility-scale PV sites located in the Bay Area, LA, Desert and San Joaquin Valley. Overall, IR CMV forecasts were more accurate than NDFD forecasts at inland CA locations when cloudy sky conditions were present. Clear sky bias was very similar for both IR CMV and NDFD forecasts in most regions. Seasonal forecast accuracy was also scrutinized in all four regions with results falling in line with expected cloud conditions. However, the IR CMV forecasts were shown to be less accurate than NDFD forecasts when marine stratus clouds were present due to IR satellite image cloud detection limitations. To address this limitation, two experimental UCSD-led solar irradiance forecasting models were examined and improved upon: the WRF-SolarCA model and the ODML model.

Initial WRF-SolarCA forecasts were shown to be less accurate than CMV and NDFD forecasts. The WRF-SolarCA forecasts exhibited significant clear sky bias which systematically reduced their accuracy. Additionally, the initial WRF-SolarCA forecasting configuration was likely minimizing cloud assimilation gains by being initialized at 5:00 PM LST when marine stratus cloud coverage tends to be near its minimum. In response, WRF-SolarCA model forecasts were retargeted at coastal marine cloud layer forecasting regimes and treated with a Cloud Data Assimilation and Well-Mixed Preprocessor scheme (WEMPPDA) and an Inversion Base Height (IBH) adjustment scheme in separate trials. WRF-WEMPPDA results demonstrated a strong positive bias, suggesting failure to predict adequate cloud cover in the coastal LA region. However, WRF-IBH demonstrated a marked improvement over uncorrected WRF results, showing low bias error, even when compared against persistence forecasts. WRF-IBH results outperform persistence forecasts in every metric except MBE_{kt}. WRF-IBH results also demonstrated high accuracy in direct PV power generation forecasts, yielding consistently lower error than NDFD, IR and visible CMV forecasts.

The ODML model was tested with increasingly relevant input. ODML-training ensemble techniques were applied to benchmark IR and visible CMV and NDFD irradiance forecasts, with moderate to significant bias correction noted under almost all conditions and locations. The highest-performing ODML model combination was composed of

forecasted GHI, DNI, and Power inputs. In individual forecast trainings, NDFD forecasts saw the greatest error reduction, with coastal region PV plants experiencing the most significant forecast improvements. Ensemble ODML trials applied to IR and visible CMV, and NDFD forecasts in tandem yielded further bias and error reduction across all PV plant sizes and locations.

The most exciting and applicable gains in this research project were in the area of California ISO load forecasting improvement. Overall, PG&E load zone ALFS-BTM DA forecasts performed better than baseline ALFS forecasts when compared to actual load data. Cloudy day ALFS-BTM forecast improvement was significant and reached as high as 18% at 2PM LST for all cloudy hours observed in this analysis. Specifically, ALFS-BTM DA forecasts were observed to have the largest reduction of error during the afternoon on cloudy days as noted in the five-day case study period. However, DA ALFS-BTM forecasts showed little or no improvement during early morning hours due to the higher morning load variability associated with the PG&E load zone.

30 minute-ahead ALFS-BTM forecasts were shown to experience improvement under all sky conditions for the SDG&E load zone, especially during the morning time periods when traditional load forecast often experience their largest uncertainties. Though less pronounced, SCE zone 30 minute-ahead ALFS-BTM forecasts showed modest improvements under cloudy sky conditions. PG&E load zone 30 minute-ahead forecasts were generally less accurate with the inclusion of associated BTM solar energy forecasts likely due to the widely varying weather conditions common across its zonal footprint. Partitioning of SCE and PG&E load zones into their respective coastal and inland sub-zones could allow for similar forecasting accuracy improvements as noted with the SDG&E regional ALFS forecasts.

All project milestones and deliverables were met and delivered on schedule except for milestone and deliverable 4.1 (ALFS load forecast accuracy comparison) which was delayed due to California ISO limitations on outside work commitments. CPR engaged directly with Itron to provide the required ALFS analysis and data generation needed for successful milestone and deliverable completion.

This overall project work culminated in a GO decision being made by the California ISO on including zonal BTM forecasts into its operational ALFS. California ISO's Manager of Short Term forecasting, Jim Blatchford, had this to say about the research performed here, "The behind-the-meter (BTM) California ISO region forecasting research performed by Clean Power Research and sponsored by the Department of Energy's SUNRISE program was an opportunity to verify value and demonstrate improved load forecast capability. In 2016, the California ISO will be incorporating the BTM forecast into the Hour Ahead and Day Ahead load models to look for improvements in the overall load forecast accuracy as BTM PV capacity continues to grow."

Budget and Schedule

Recipient:	Clean Power Research, Tom Hoff		
DOE Award #:	EE0006329		
Spending Summary for SF 424A Budget Forms			
Object Class Categories	**APPROVED BUDGET**	**TOTAL SPENT TO DATE (12/15/2015)**	**Forecasted Spending (FINAL COSTING FOR FY14 SCOPE)**
a. Personnel	$398,603	$409,508	$430,000
b. Fringe Benefits	$123,567	$126,947	$133,300
c. Travel			
d. Equipment			
e. Supplies			
f. Contractual	$334,671	$118,290	$123,460
g. Construction			
h. Other			
i. Total Direct Charges (sum of a to h)	$856,841	$654,745	$686,760
j. Indirect Charges	$196,512	$201,887	$980,400
k. Totals (sum of i and j)	**$1,053,353**	**$856,632**	**$1,667,160**
DOE Share	$500,000	$406,892	$500,000
Cost Share	$553,353	$449,740	$1,167,160
Calculated Cost Share Percentage	52.5%	52.5%	70.0%

Path Forward

Accurate simulation under challenging weather conditions impacting fleet-scale PV energy production is difficult at best. Widely varying weather phenomena, such as coastal marine stratus and mid-summer monsoon clouds, present significant challenges to current CMV and NWP forecasts. Increasing this challenge is the difficulty of simulating individual PV system performance without introducing additional forecast errors. Future work will address these challenges, including additional refinements of IR-based satellite cloud detection algorithms and further investigation of WRF-IBH forecasting options.

A separate focus for future work will be optimization of forecast blending using machine learning. As Dr. Coimbra's ODML studies at UCSD demonstrated, training applied to CMV and NWP model forecasts in tandem produced maximum reduction in forecast error. Application of ODML training to on-the-fly blended forecasts is a valuable future goal in further improving forecast accuracy.

The most significant future work is improving California ISO's ALFS accuracy by further incorporating BTM into load forecasts. CPR will continue to work with California ISO to update the current BTM fleet database, further evaluate and improve BTM forecast accuracy, and optimize computation speed for BTM forecast simulations.

If realistic goals are met by reducing variance in satellite-based forecasts, utilizing cutting-edge technology to optimize blending of CMV forecasts with numerical models, and consolidating and updating PV fleet data, irradiance and load forecasting will become more accurate than ever before.

References

Hammer, A., D. Heinemann, C. Hoyer and E. Lorenz, 2001: "Satellite Based Short-Term Forecasting of Solar Irradiance - Comparison of Methods and Error Analysis", *Proc. EUMETSAT Meteorological Satellite Data Users Conf.*

Israel Lopez-Coto, Patrick Mathiesen, Juan Luis Bosch, Brian D'Agostino, Brandt Maxwell, Robert Fovell and Jan Kleissl, "A Comparison between Several Parameterization Schemes in WRF for Solar Forecasting in Coastal Southern California", submitted to *Monthly Weather Review*, 2014.

Kaur, A., H.T.C. Pedro and C.F.M. Coimbra, 2013 "Impact of Onsite Solar Generation on System Load Demand Forecast", *Energy Conversion and Management*, **75**, 701-709.

Lorenz, E., D. Heinemann and A. Hammer, 2004: Short-term Forecasting of Solar Radiation Based on Satellite Data. *Proc. Eurosun (ISES Europe Solar Congress)*, Freiburg, Germany.

Mathiesen, P., and J. Kleissl, 2011: "Evaluation of numerical weather prediction for intra-day solar forecasting in the continental United States", *Solar Energy* **85**, 967-977.

Mathiesen, P., C. Collier, and J. Kleissl, 2013: "A high-resolution, cloud-assimilating numerical weather prediction model for solar irradiance forecasting". *Solar Energy,* **92**, 47-61.

Perez, R., P. Ineichen, K. Moore, M. Kmiecikm, C. Chain, R. George and E. Vignola, 2002: "A New Operational Satellite-to-Irradiance Model", *Solar Energy*, vol. **73**, 307-317.

Perez, R., S. Kivalov, J. Schlemmer, K. Hemker Jr., D. Renné, and T.E. Hoff, 2010: "Validation of short and medium term operational solar radiation forecasts in the US", *Solar Energy*, vol. **84**, 2161-2172.

Tuohy, A., J. Zack, S. Haupt, J. Sharp, M. Ahlstrom, S. Dise, E. Grimit, C. Möhrlen, M. Lange, M. Garcia Casado, J. Black, M. Marquis, and C. Collier, 2015: "Solar forecasting: Methods, challenges, and performance", *IEEE Power & Energy Magazine*, **13**, 50-59

Zhong, X., and J. Kleissl, 2015: "Clear sky irradiances using REST2 and MODIS," *Solar Energy*, vol. **116**, 144-164.